From nano to macro: Introduction to atomistic modeling techniques

IAP 2007

Nanomechanics of hierarchical biological materials *(cont'd)*

Size Effects in Deformation of Materials

Lecture 8

Department of
Civil & Environmental Engineering
Massachusetts Institute of Technology

Markus J. Buehler

Outline

1. **Introduction to Mechanics of Materials**
   Basic concepts of mechanics, stress and strain, deformation, strength and fracture
   Monday Jan 8, 09-10:30am
2. **Introduction to Classical Molecular Dynamics**
   Introduction into the molecular dynamics simulation; numerical techniques
   Tuesday Jan 9, 09-10:30am
3. **Mechanics of Ductile Materials**
   Dislocations; crystal structures; deformation of metals
   Tuesday Jan 16, 09-10:30am
4. **The Cauchy-Born rule**
   Calculation of elastic properties of atomic lattices
   Friday Jan 19, 09-10:30am
5. **Dynamic Fracture of Brittle Materials**
   Nonlinear elasticity in dynamic fracture, geometric confinement, interfaces
   Wednesday Jan 17, 09-10:30am
6. **Mechanics of biological materials**
   Monday Jan. 22, 09-10:30am
7. **Introduction to The Problem Set**
   Atomistic modeling of fracture of a nanocrystal of copper.
   Wednesday Jan 22, 09-10:30am
8. **Size Effects in Deformation of Materials**
   Size effects in deformation of materials: Is smaller stronger?
   Friday Jan 26, 09-10:30am

Typical simulation procedure

1. Pre-processing (define geometry, build crystal etc.)
2. Energy relaxation (minimization)
3. Annealing (equilibration at specific temperature)
4. “Actual” calculation; e.g. apply loading to crack
5. Analysis

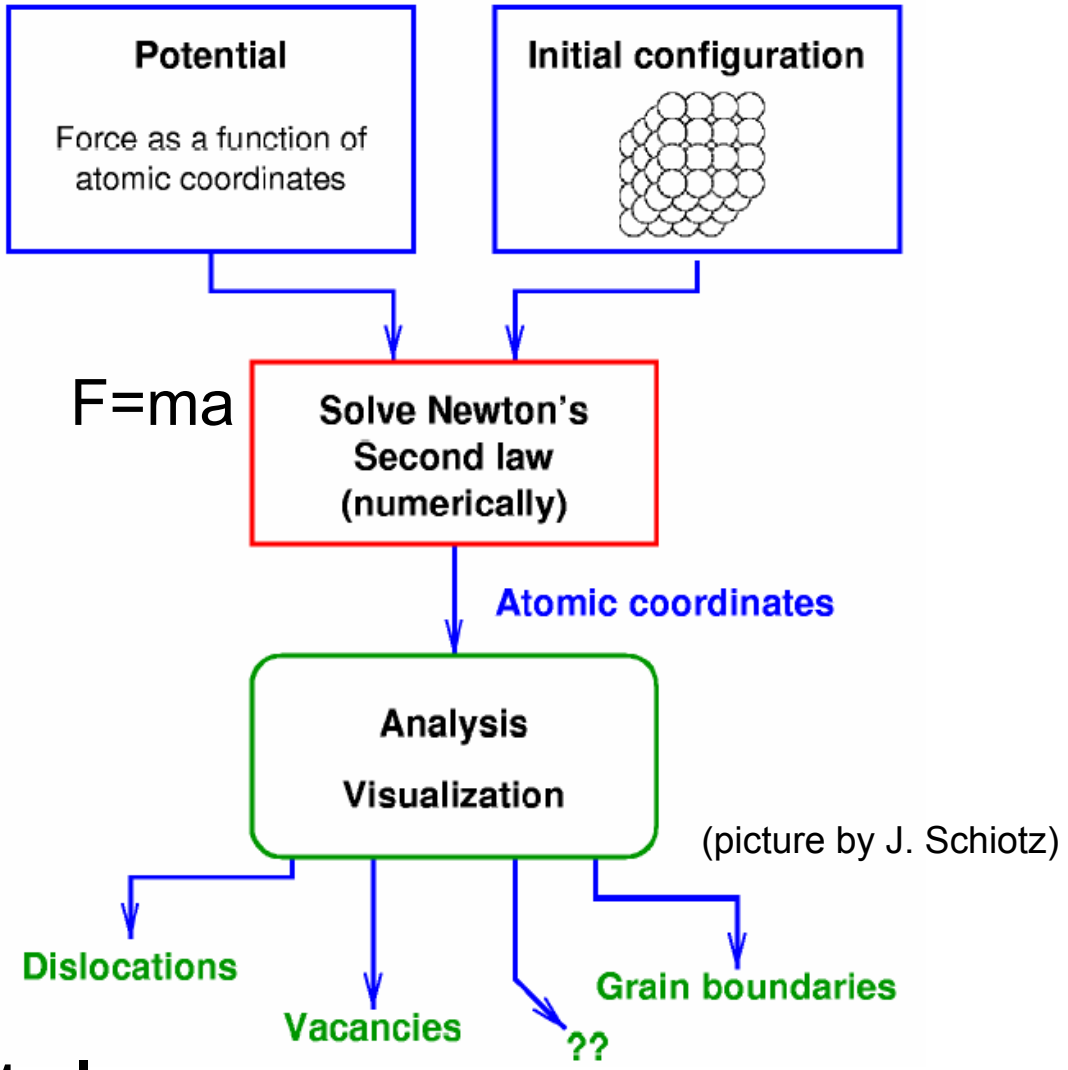

(picture by J. Schiotz)

Real challenge:
Questions to ask and what to learn

Common empirical force fields

Class I (experiment derived, simple form)

- CHARMM
- CHARMm (Accelrys)
- AMBER
- OPLS/AMBER/Schrödinger
- ECEPP (free energy force field)
- GROMOS

Harmonic terms; Derived from vibrational spectroscopy, gas-phase molecular structures
Very system-specific

Class II (more complex, derived from QM)

- CFF95 (Biosym/Accelrys)
- MM3
- MMFF94 (CHARMM, Macromodel…)
- UFF, DREIDING

Include anharmonic terms
Derived from QM, more general

Image removed due to copyright restrictions.

http://www.ch.embnet.org/MD_tutorial/pages/MD.Part2.html
http://www.pharmacy.umaryland.edu/faculty/amackere/force_fields.htm
http://amber.scripps.edu/

Alpha helix and beta sheets

Hydrogen bonding

e.g. between O and H in H_2O

Between N and O in proteins…

Images removed due to copyright restrictions.

Image removed due to copyright restrictions.

Image removed due to copyright restrictions.
See: http://www.columbia.edu/cu/biology/courses/c2005/images/3levelpro.4.p.jpg

Unfolding of alpha helix structure

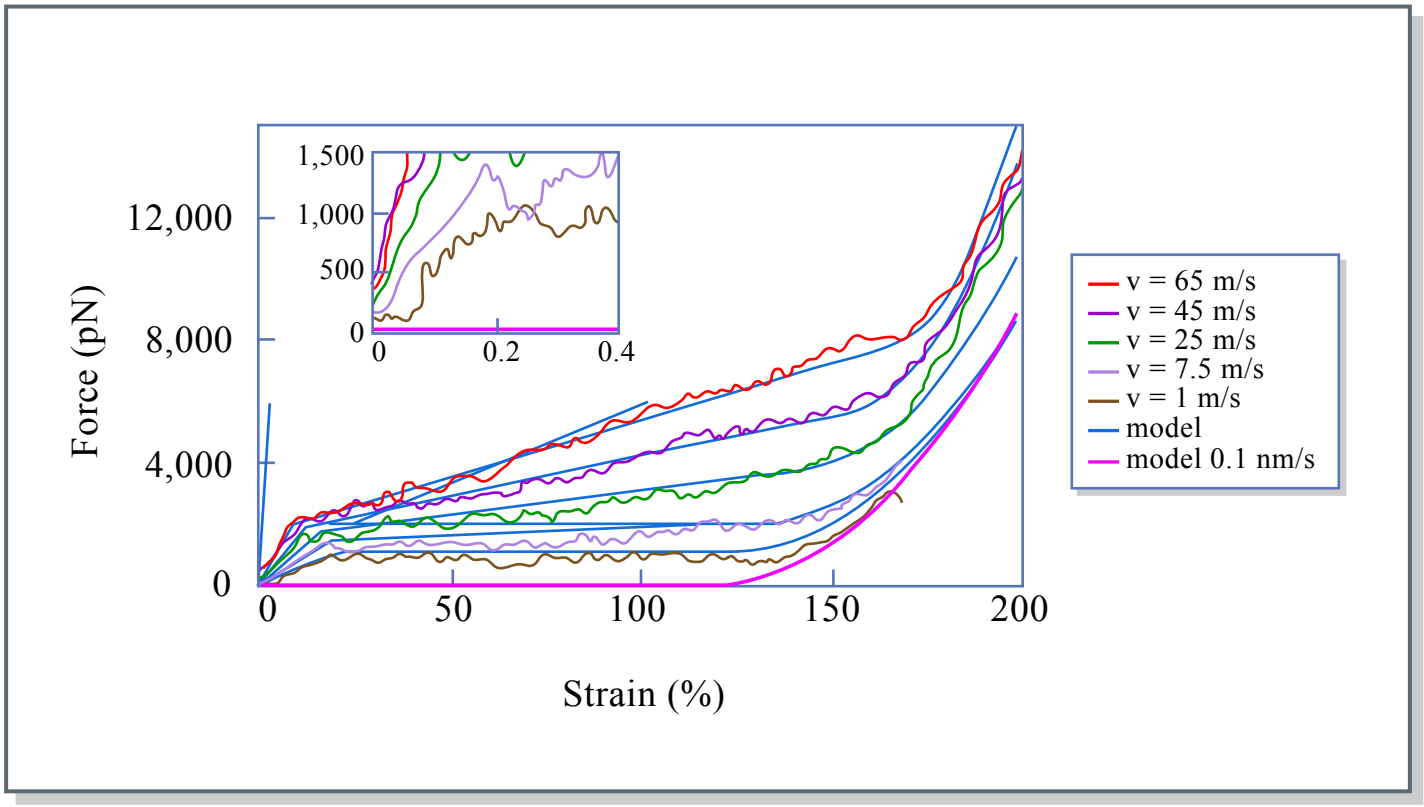

Figure by MIT OCW. After Ackbarow and Buehler, 2007.

Ackbarow and Buehler, 2007

Unfolding of beta sheet

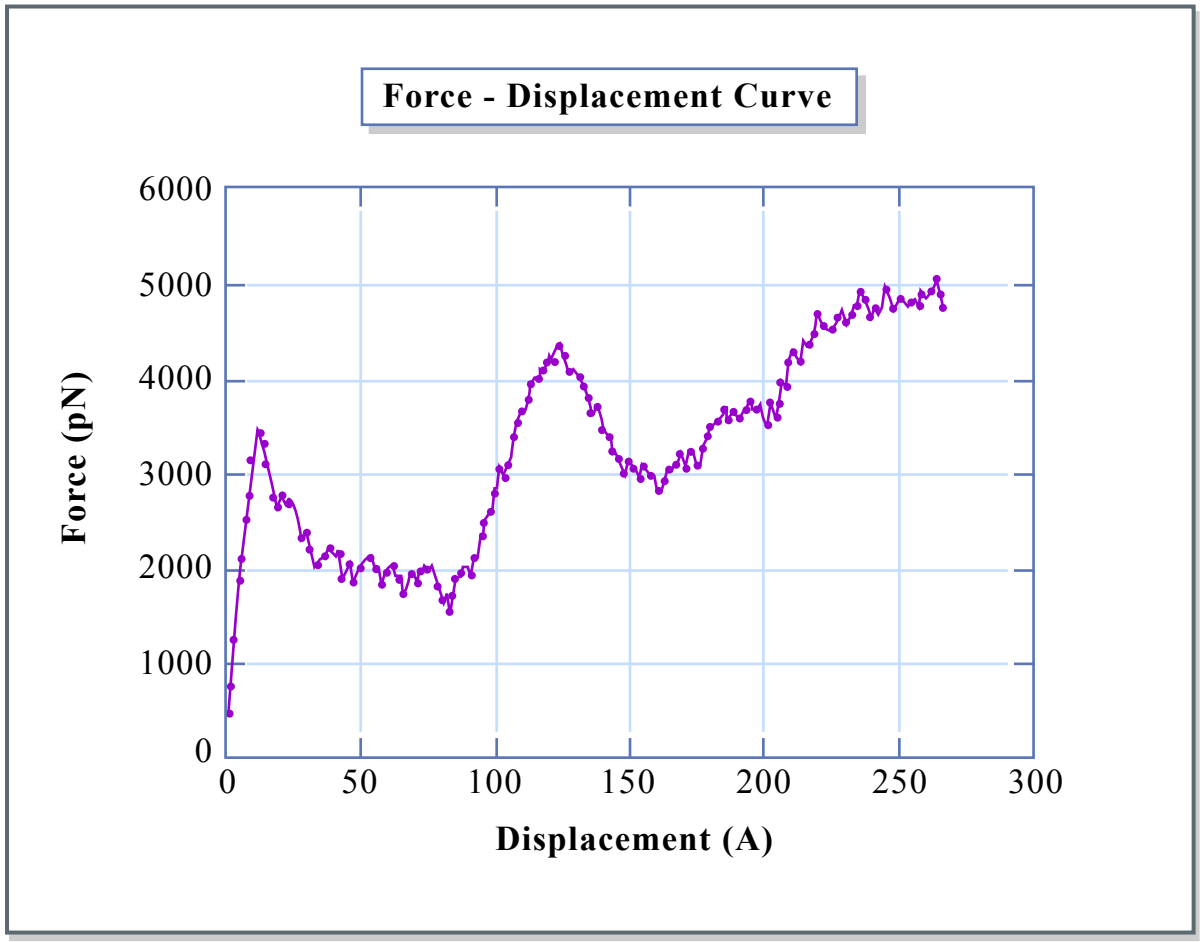

Figure by MIT OCW.

Titin I27 domain: Very resistant to unfolding due to parallel H-bonded strands

Image removed due to copyright restrictions.

Keten and Buehler, 2007

Stretching experiment: Tropocollagen molecule

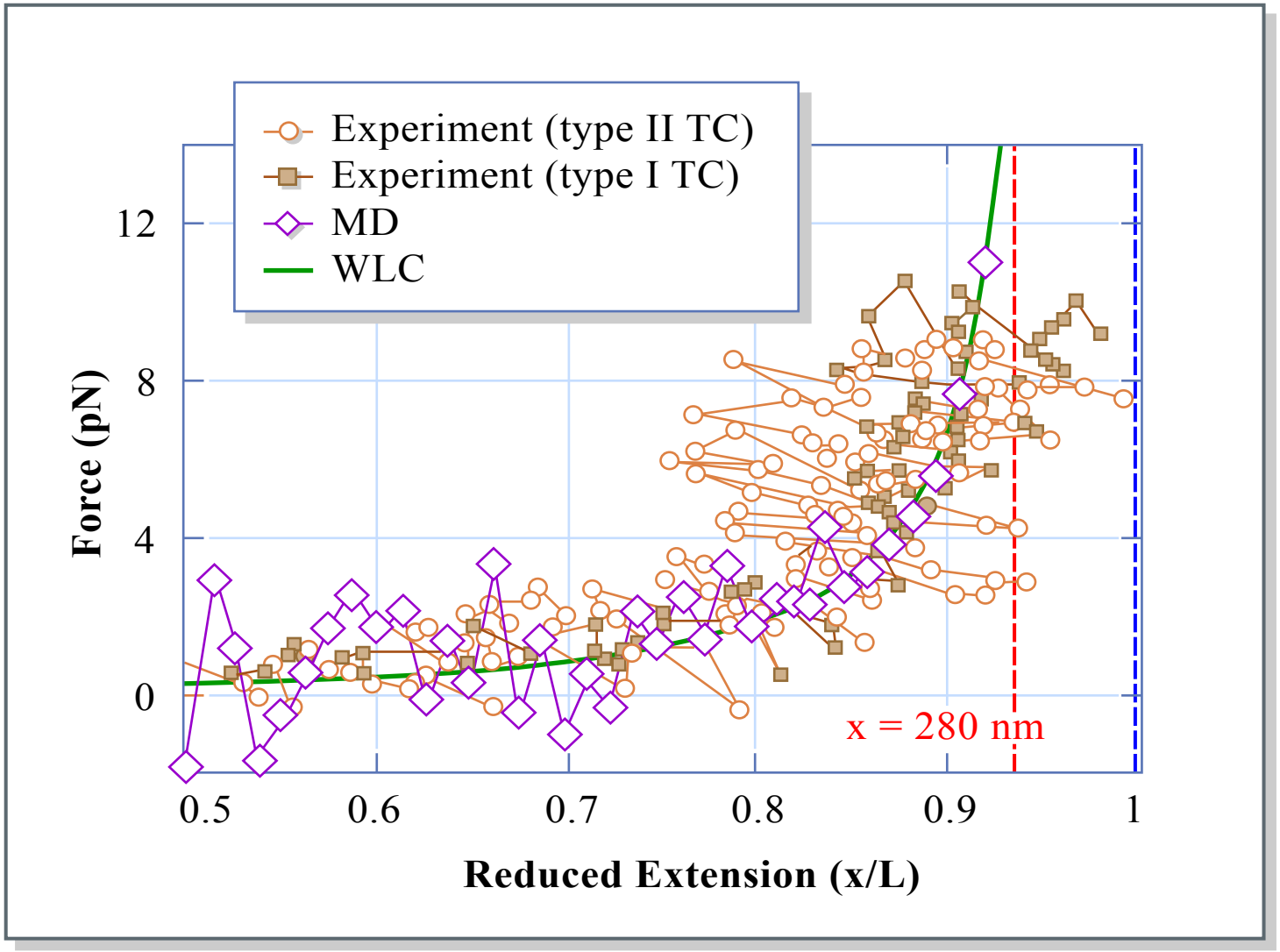

Figure by MIT OCW. After Buehler and Wong.

Fracture at ultra small scales

Size effects

Nano-scale fracture

- Failure mechanism of ultra small brittle single crystals as a function of material size
- Properties of adhesion systems as a function of material size: Is Griffith's model for crack nucleation still valid at nanoscale?

"Nano"

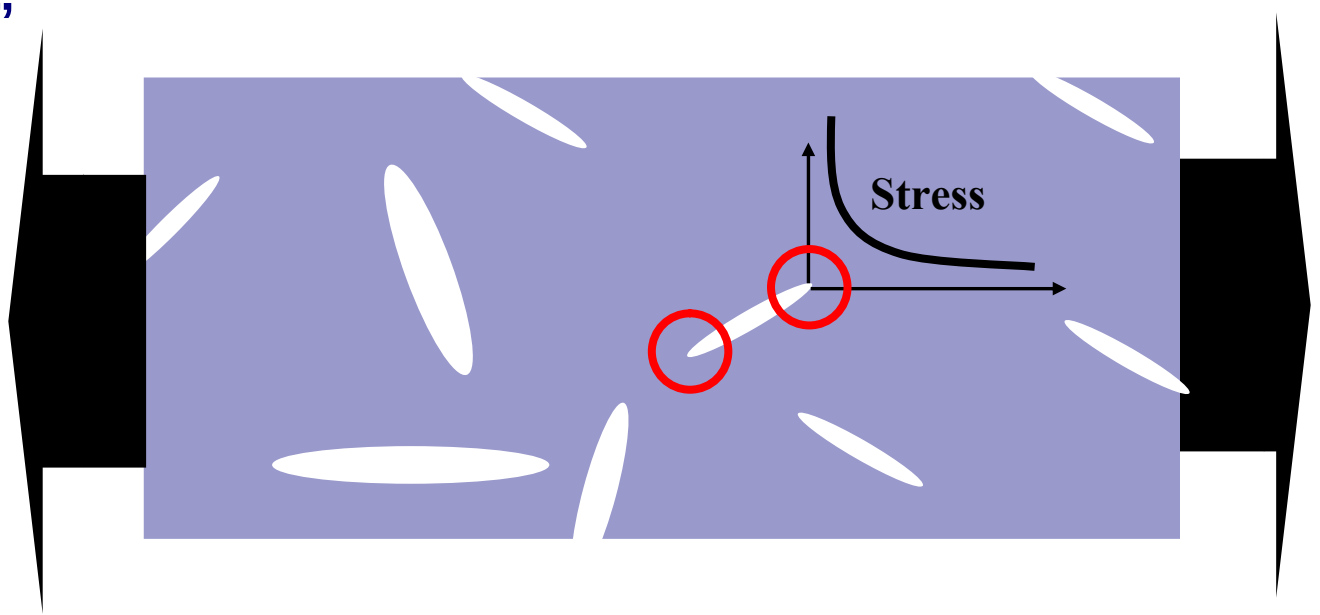

Griffith

Review: Two paradoxons of classical fracture theories

Infinite peak stress

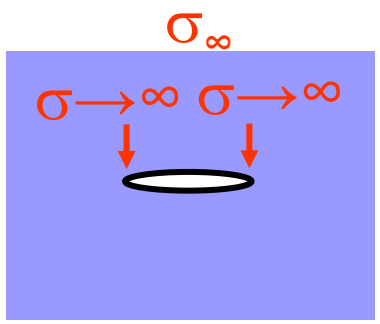

$$\sigma_{yy} = \sigma_0^* \left(1 + 2\sqrt{\frac{a}{\rho}} \right)$$

- Inglis (~1910): Stress infinite close to a elliptical inclusion once shape is crack-like

"Inglis paradox": Why does crack not extend, despite infinitely large stress at even small applied load?

- Resolved by Griffith (~ 1950): Thermodynamic view of fracture

$$G = 2\gamma$$

"Griffith paradox": Fracture at small length scales? Critical applied stress for fracture infinite in small (nano-)dimensions (ξ=O(nm))!

Considered here

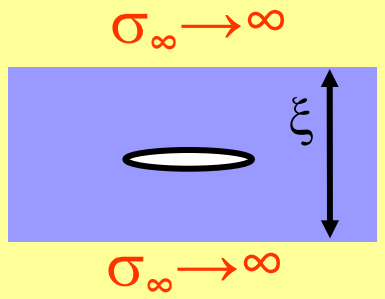

Infinite bulk stress

Buehler *et al.*, *MRS Proceedings*, 2004 & MSMSE, 2005; Gao, Ji, Buehler, *MCB*, 2004

Thin strip geometry

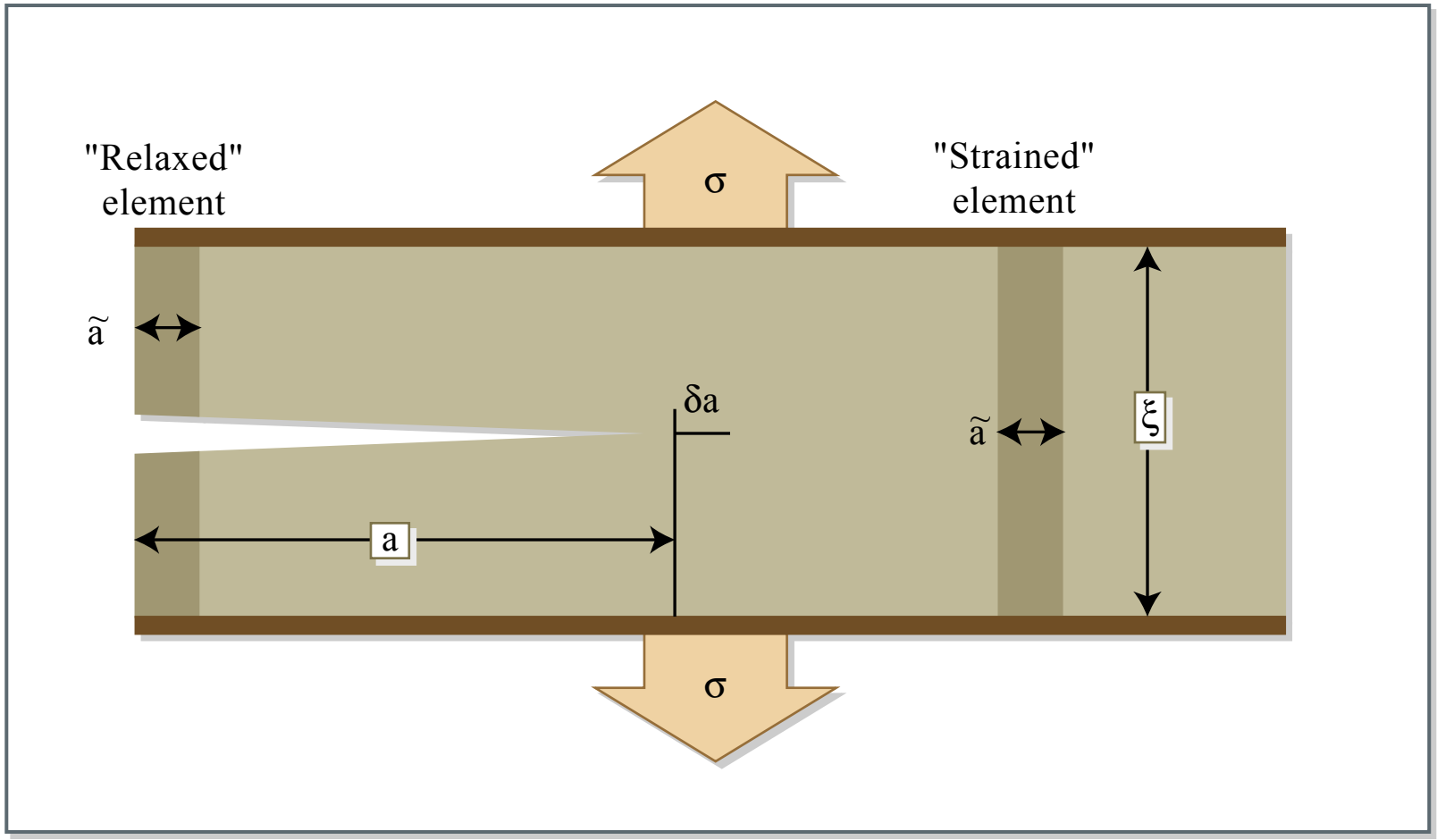

Figure by MIT OCW.

Change in potential energy: Create a "relaxed" element from a "strained" element, per unit crack advance

$$W_P = W_P(\sigma, a, \ldots)$$

Thin strip geometry

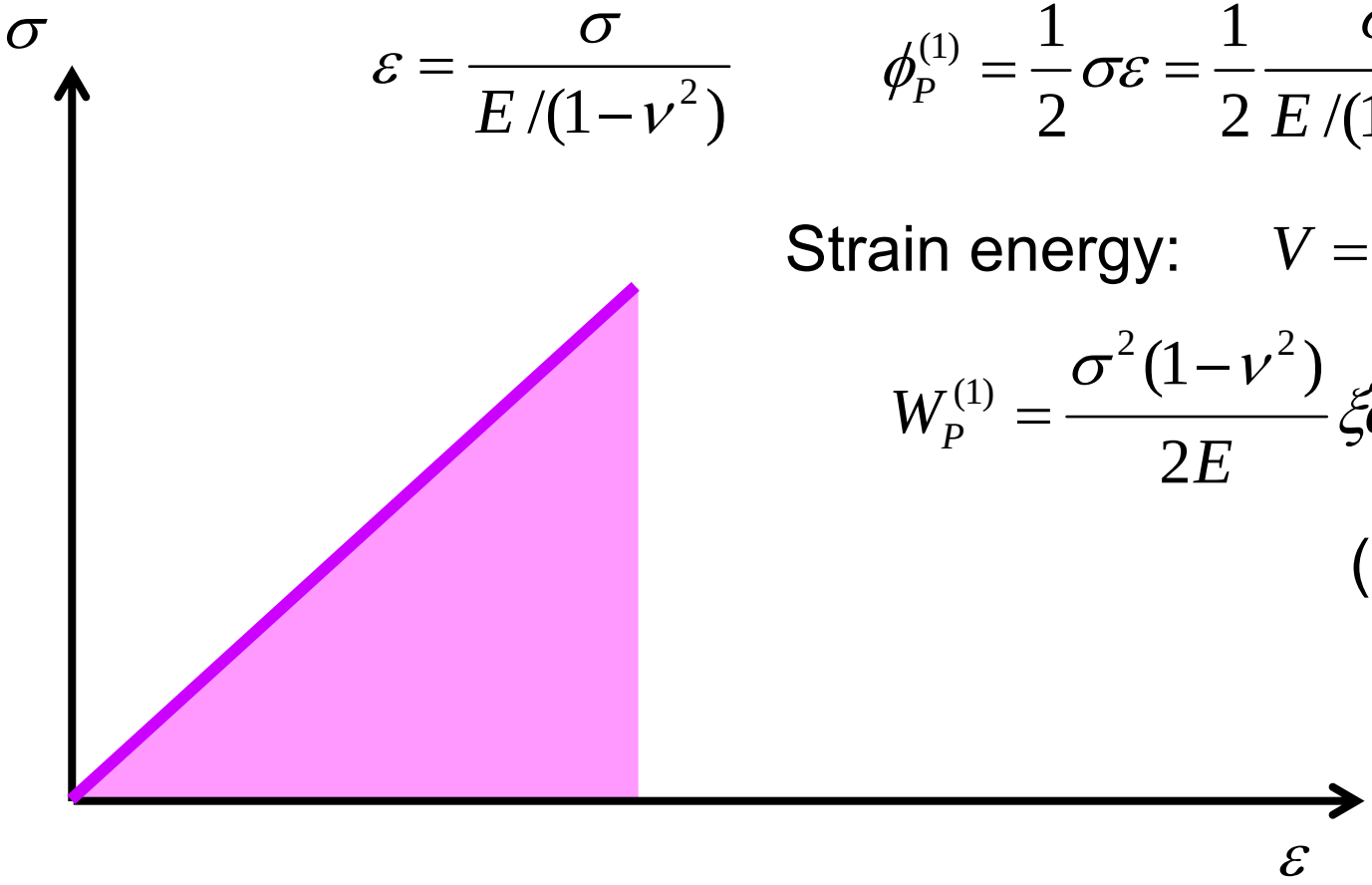

$$\varepsilon = \frac{\sigma}{E/(1-\nu^2)}$$

Strain energy density:

$$\phi_P^{(1)} = \frac{1}{2}\sigma\varepsilon = \frac{1}{2}\frac{\sigma^2}{E/(1-\nu^2)}$$

Strain energy: $V = \xi \tilde{a} B$

$$W_P^{(1)} = \frac{\sigma^2(1-\nu^2)}{2E}\xi \tilde{a} B$$

(plane strain)

Thin strip geometry

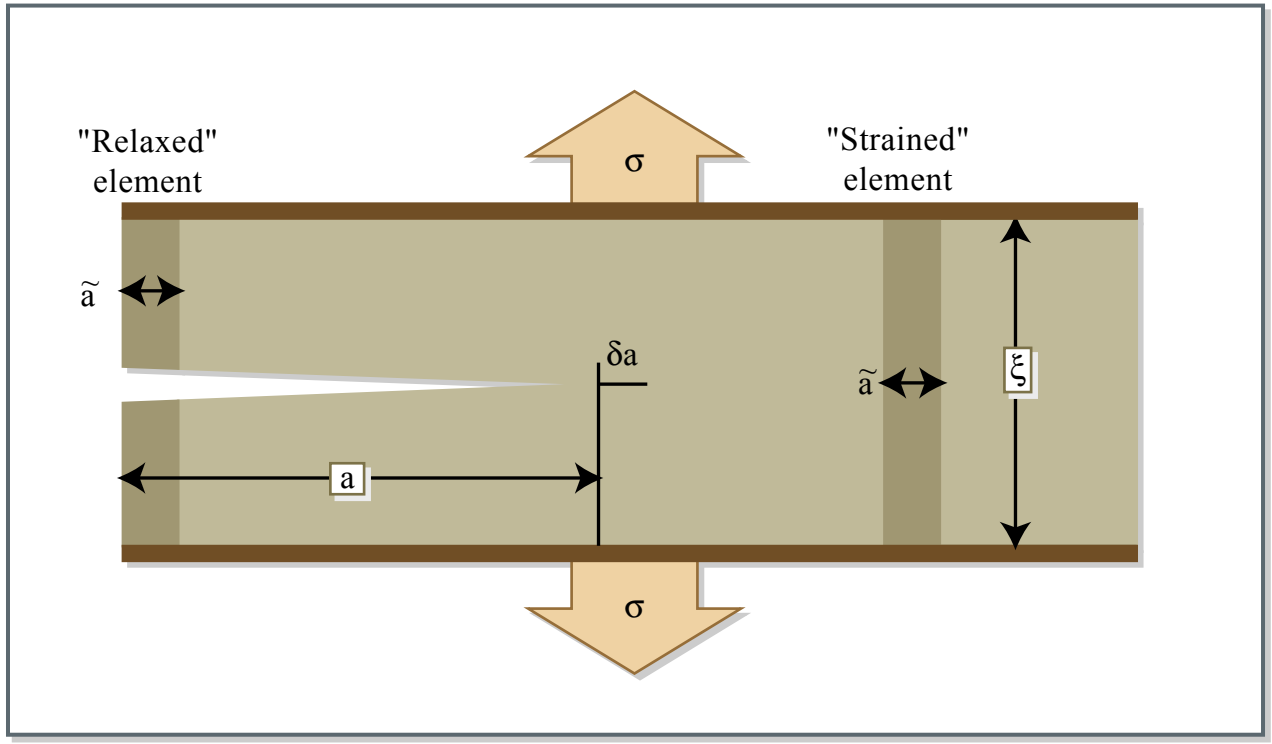

Figure by MIT OCW.

$$W_P^{(2)} = 0$$

$$W_P^{(1)} = \frac{\sigma^2(1-\nu^2)}{2E}\xi\tilde{a}B$$

$$W_P = W_P^{(2)} - W_P^{(1)} = -\frac{\sigma^2(1-\nu^2)}{2E}\xi aB$$

$$G = \frac{\sigma^2\xi(1-\nu^2)}{2E}$$

Fracture of thin strip geometry
Theoretical considerations

$$G = \frac{\sigma^2 \xi (1-\nu^2)}{2E} \qquad 2\gamma = G \quad \text{Griffith}$$

E Young's modulus
ν Poisson ratio, and
σ Stress far ahead of the crack tip

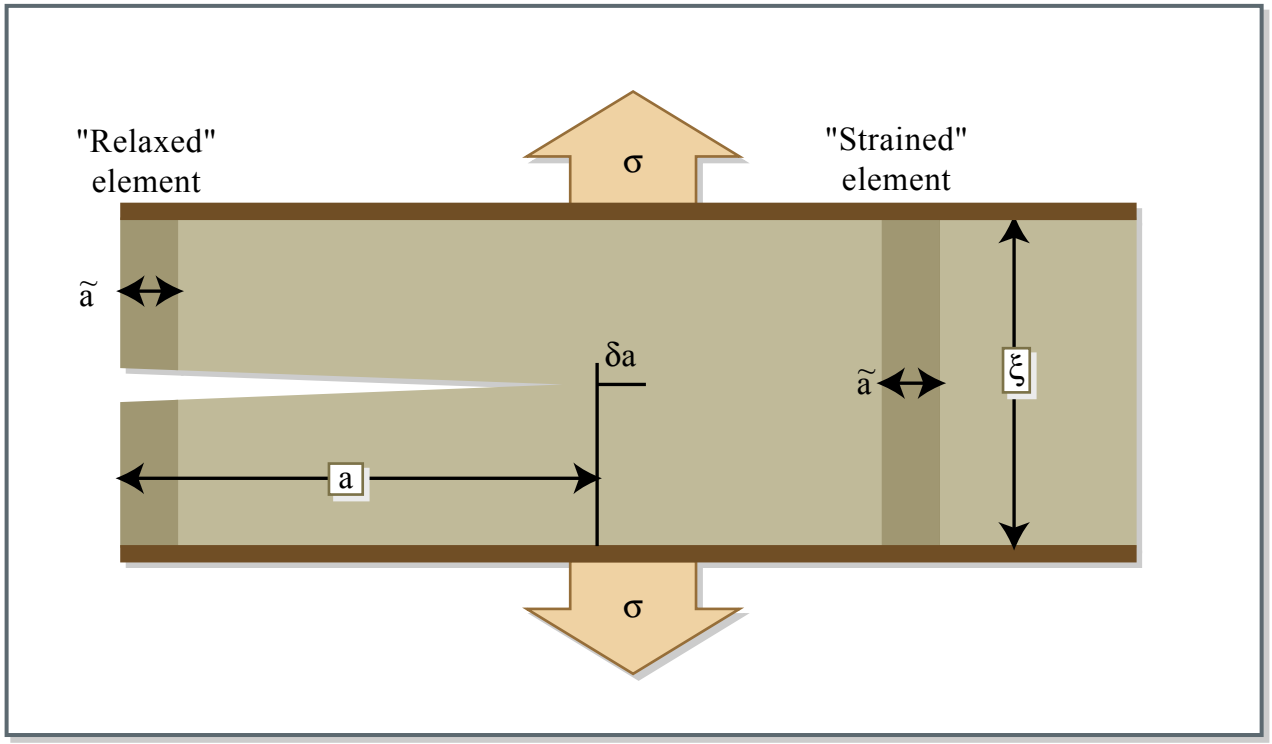

Figure by MIT OCW.

ξ.. size of material

Fracture of thin strip geometry
Theoretical considerations

Stress for spontaneous crack propagation

$$\sigma_f = \sqrt{\frac{4\gamma E}{\xi(1-\nu^2)}}$$

$\sigma \rightarrow \infty$ for $\xi \rightarrow 0$

Impossible: $\sigma_{max}=\sigma_{th}$

Length scale ξ_{cr} at σ_{th} cross-over

$$\xi_{cr} = \frac{4\gamma E}{\sigma_{th}^2(1-\nu^2)}$$

ξ.. size of material

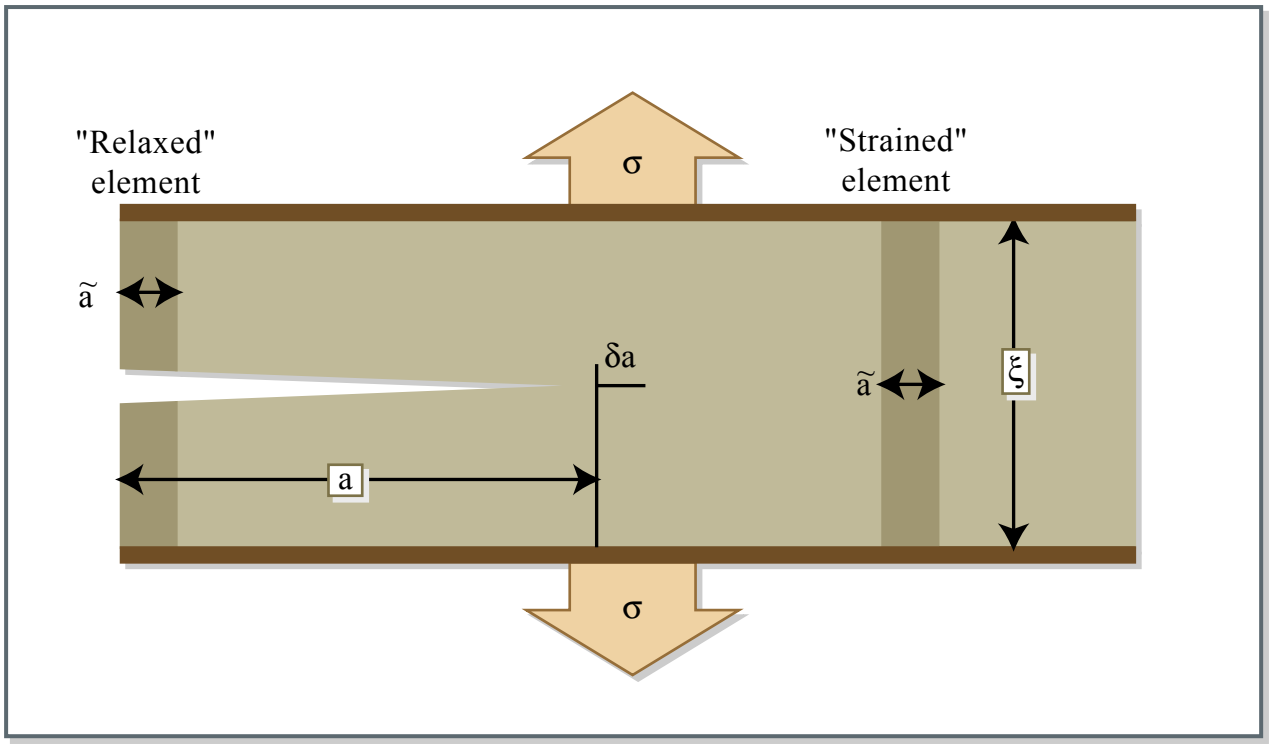

Figure by MIT OCW.

Buehler *et al.*, *MRS Proceedings*, 2004 & MSMSE, 2005; Gao, Ji, Buehler, *MCB*, 2004

Breakdown of Griffith at ultra small scales

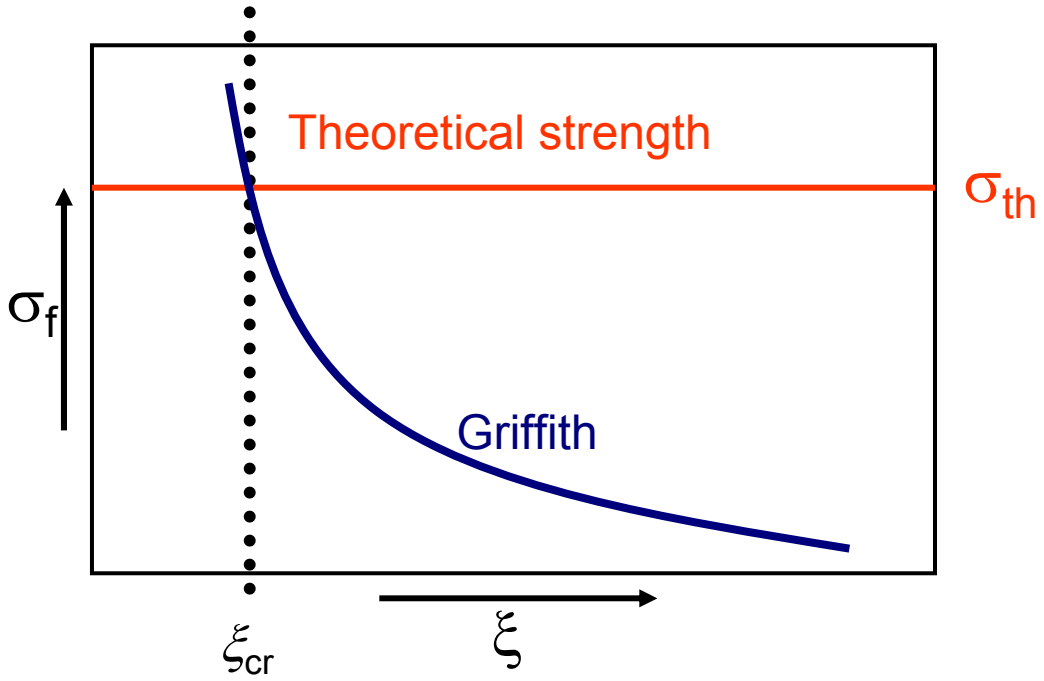

$$\xi_{cr} \sim \frac{\gamma E}{\sigma_{\max}^2}$$

Transition from Griffith-governed failure to maximum strength of material

- Griffith theory breaks down below a critical length scale
- Replace Griffith concept of energy release by failure at homogeneous stress

Atomistic model

Bulk (harmonic, FCC)

$$\phi(r) = a_0 + \frac{1}{2} k_0 (r - r_0)^2 \qquad r_0 = 2^{1/6} \qquad k_0 = 572.0$$

$$a \approx 1.587$$

$$\mu = \frac{r_0^2}{2} k_0 \qquad E = 8/3\mu \qquad \nu = 1/3$$

$$h_{cr} = \frac{4\gamma E}{\sigma_{th}^2 (1-\nu^2)}$$

Interface (LJ) "dispersive-glue interactions"

$$\phi(r) = 4\varepsilon\left(\left(\frac{\sigma}{r}\right)^{12} - \left(\frac{\sigma}{r}\right)^{6}\right) \qquad \varepsilon = \sigma = 1$$

$$\gamma = N_b \rho_A \Delta\phi \qquad \sigma_{th} \approx 9.3$$

$$\rho_A = 1/r_0^2 \approx 0.794$$

$$N_b = 4 \qquad \Delta\phi \approx 1$$

Forces by dϕ/dr

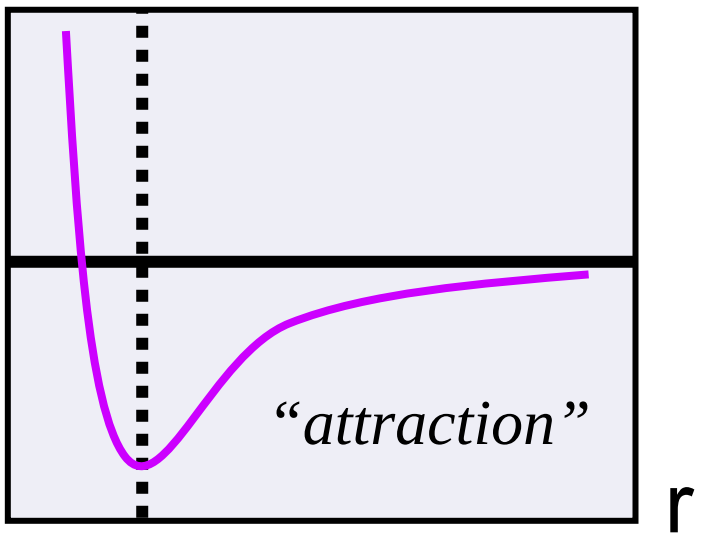

Choose *E* and γ such that length scale is in a regime easily accessible to MD

Atomistic simulation results

$\sigma_f = \sigma_{th}$ Failure at theor. strength

$$\sigma_f = \sqrt{\frac{4\gamma E}{h(1-\nu^2)}}$$

Griffith-governed failure

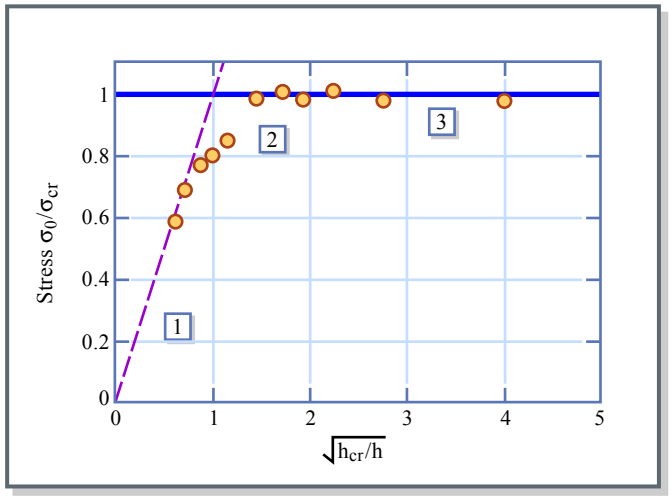

Figure by MIT OCW.

$$\xi_{cr} = \frac{4\gamma E}{\sigma_{th}^2(1-\nu^2)}$$

Atomistic simulation indicates:

➢ At critical **nanometer-length scale**, structures become insensitive to flaws: Transition from Griffith governed failure to failure at theoretical strength, independent of presence of crack!!

(Buehler *et al.*, *MRS Proceedings*, 2004; Gao, Ji, Buehler, *MCB*, 2004)

Stress distribution ahead of crack

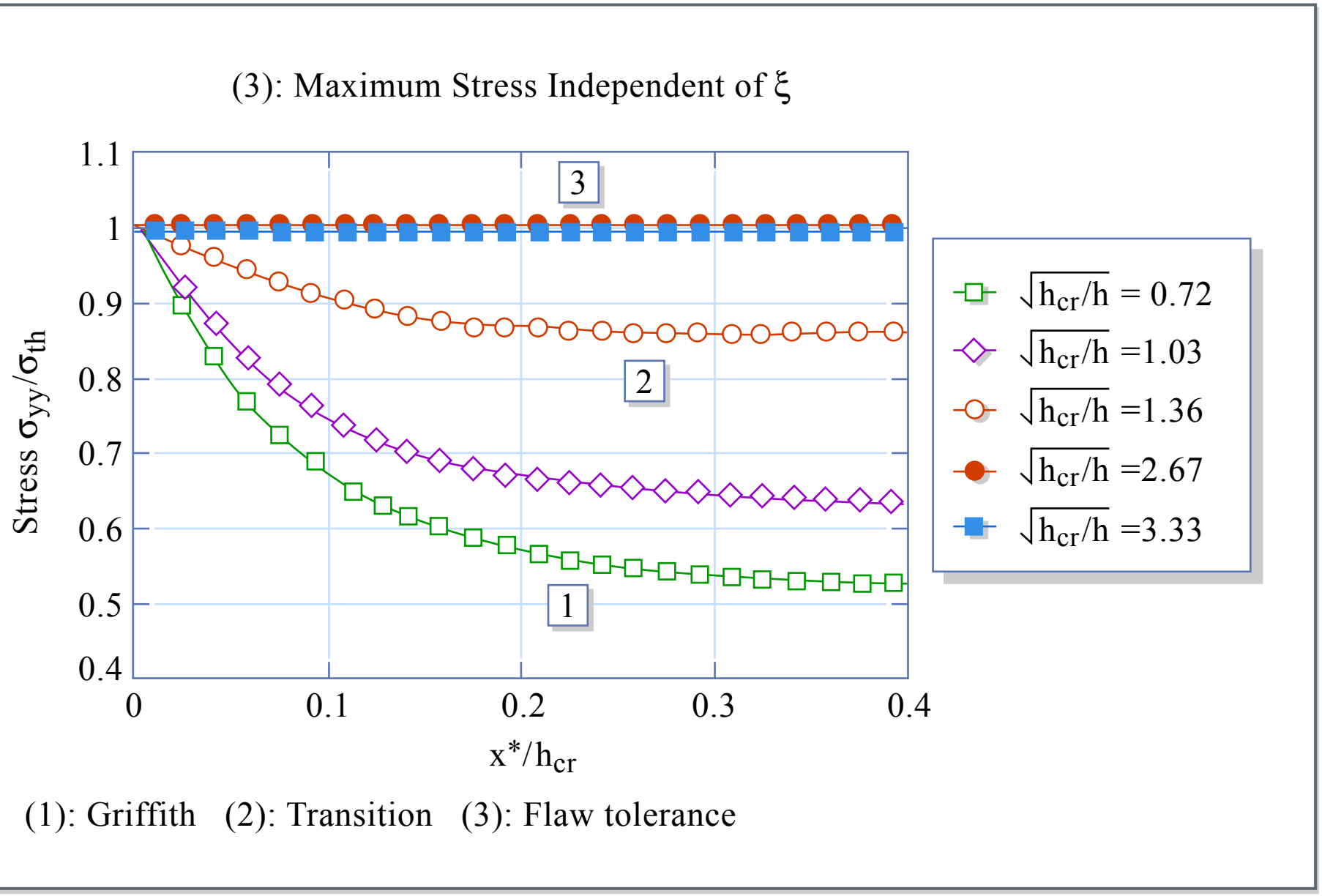

Figure by MIT OCW.

Summary: Small-scale structures for strength optimization & flaw tolerance

$$h_{cr} \propto \frac{\gamma E}{\sigma_{\max}^{2}}$$

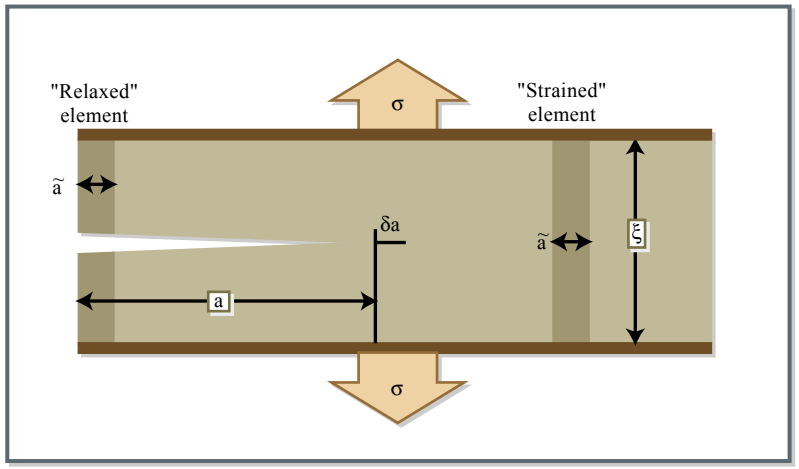

Figure by MIT OCW.

$h > h_{cr}$	$h < h_{cr}$
Material is sensitive to flaws.	Material becomes insensitive to flaws.
Material fails by stress concentration at flaws.	There is no stress concentration at flaws. Material fails at theoretical strength.
Fracture strength is sensitive to structural size.	Fracture strength is insensitive to structure size.

(Gao *et al.*, 2004; Gao, Ji, Buehler, MCB, 2004)

Can this concept explain the design of biocomposites in bone?

Characteristic size: 10..100 nm

Image removed due to copyright restrictions.

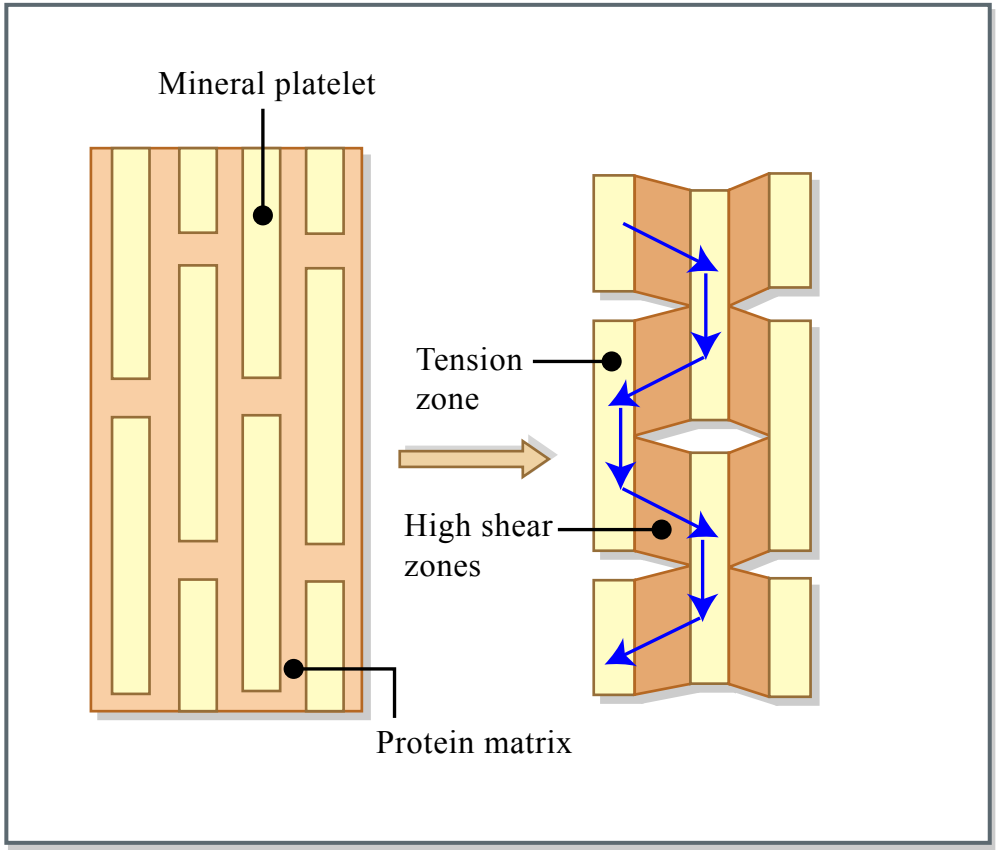

Figure by MIT OCW.

Estimate for biominerals:

$$\sigma_{\max} \approx \frac{E}{30}, \ \nu \approx 0.25, \ E = 100 \text{ GPa}, \ \gamma = 1 \text{J/m}^2$$

$$\Psi^* \approx 0.022 \qquad h_{cr} \approx 30 \text{ nm}$$

(Gao *et al.*, 2003, 2004)

Adhesion of Geckos

Autumn et al., PNAS, 2002

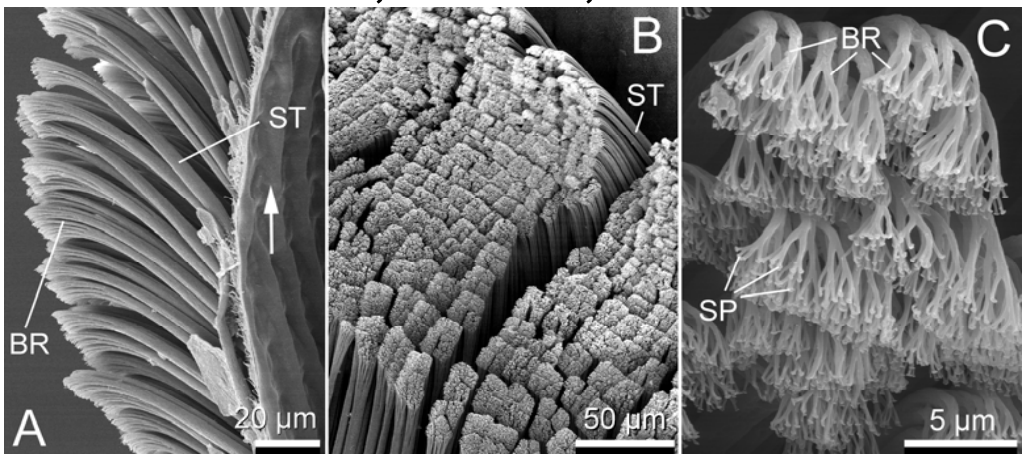

Courtesy of National Academy of Sciences, U.S.A. Used with permission.
Source: Autumn, Kellar, Metin Sitti, Yiching A. Liang, Anne M. Peattie, Wendy R. Hansen, Simon Sponberg, Thomas W. Kenny, Ronald Fearing, Jacob N. Israelachvili, and Robert J. Full. "Evidence for van der Waals adhesion in gecko setae." *PNAS* 99 (2002): 12252-12256.
(c) National Academy of Sciences, U.S.A.

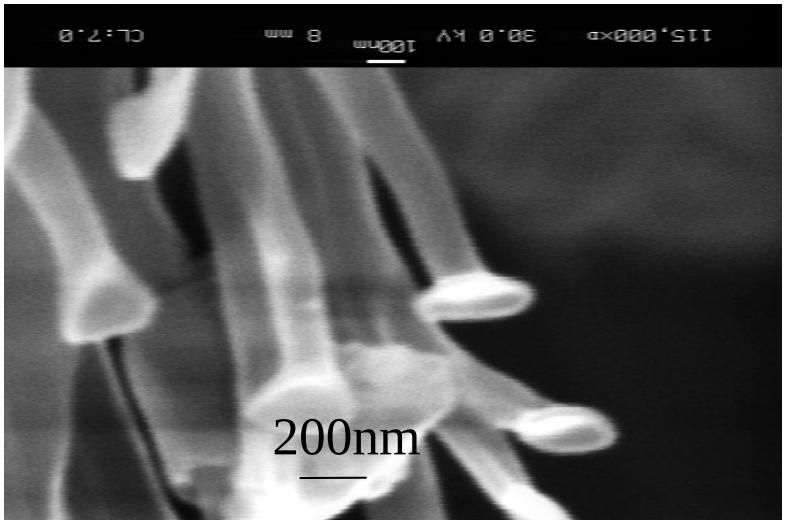

Image removed due to copyright restrictions.

Adhesion at small length scales

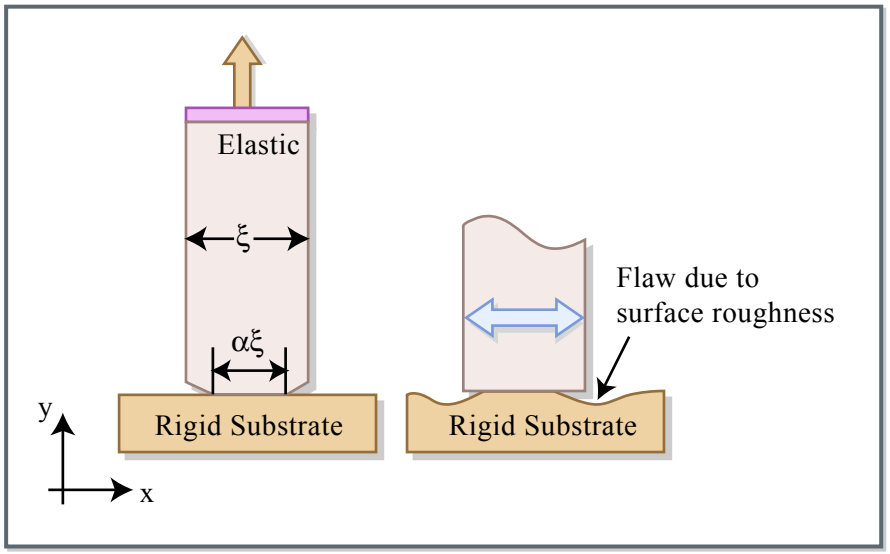

Image removed due to copyright restrictions.

(S. Gorb)

Figure by MIT OCW.

Strategies to increase adhesion strength

-Since F ~ gR (JKR model), increase line length of surface by contact splitting (Arzt *et al*., 2003)

-At very small length scales, nanometer design results in optimal adhesion strength, independent of flaws and shape (Gao *et al*., 2004)

• Schematic of the model used for studies of adhesion: The model represents a cylindrical Gecko spatula with radius attached to a rigid substrate.

• A circumferential crack represents flaws for example resulting from surface roughness. The parameter denotes the dimension of the crack.

Equivalence of adhesion and fracture problem

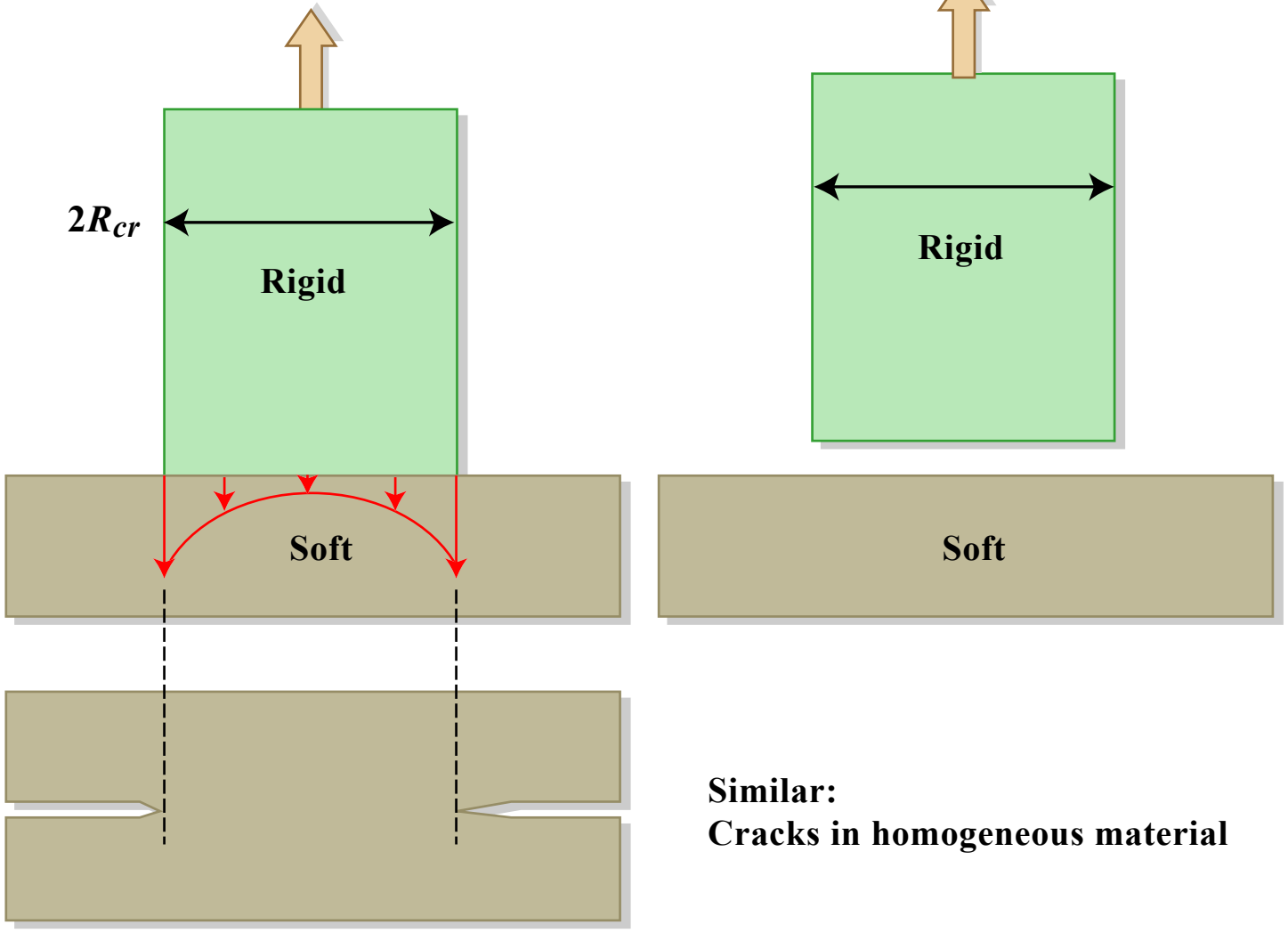

Figure by MIT OCW.

Equivalence of adhesion and fracture problem

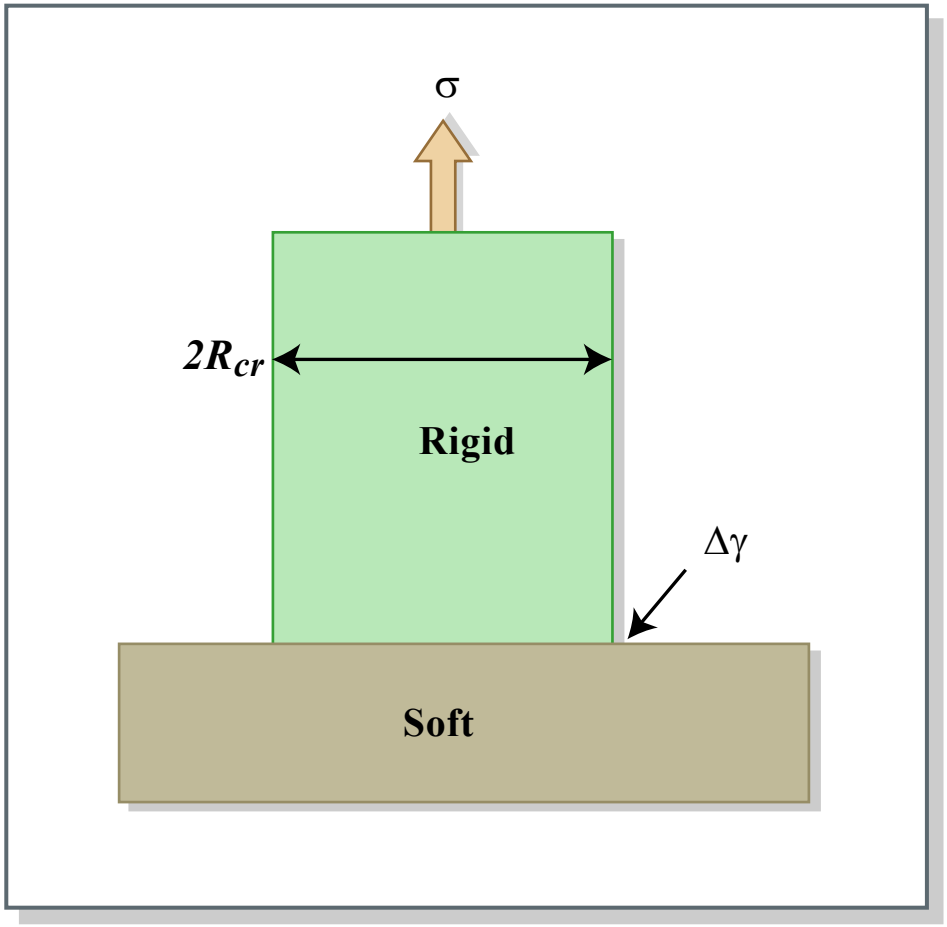

Figure by MIT OCW.

Energy release rate $K_I = \sqrt{\frac{\pi}{8} R_{cr} \sigma^2}$

$$G = \frac{K_I^2}{E'} = \frac{\pi}{8} \frac{R_{cr}}{E'} \sigma^2$$

$$G = 2\gamma = \Delta\gamma$$

Adhesion energy

Theoretical considerations
Adhesion problem as fracture problem

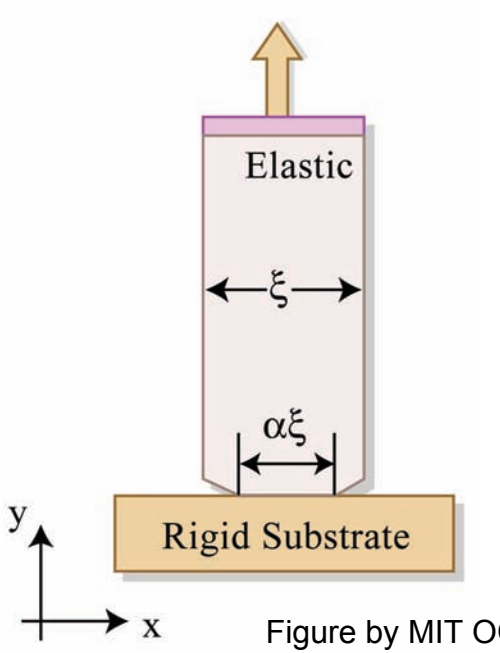

Figure by MIT OCW.

Function (tabulated)

$$K_I = \frac{P}{\pi a^2}\sqrt{\pi a}\,F_1(\alpha)$$

$$\frac{K_I^2}{2E^*} = \Delta\gamma$$

$$\beta = \sqrt{2/\left(\pi\alpha F_1^{\,2}(\alpha)\right)}$$

$$E^* = E/(1-\nu^2)$$

$$R_{cr} = \beta^2 \frac{\Delta\gamma E^*}{\sigma_{th}^2}$$

$$R_{cr} \sim 225nm$$

Typical parameters for Gecko spatula

Continuum and atomistic model

Three-dimensional model

Cylindrical attachment device

$$\phi(r) = a_0 + \frac{1}{2}k_0(r - r_0)^2$$

Harmonic

$$\phi(r) = 4\varepsilon\left(\left(\frac{\sigma}{r}\right)^{12} - \left(\frac{\sigma}{r}\right)^{6}\right)$$

LJ

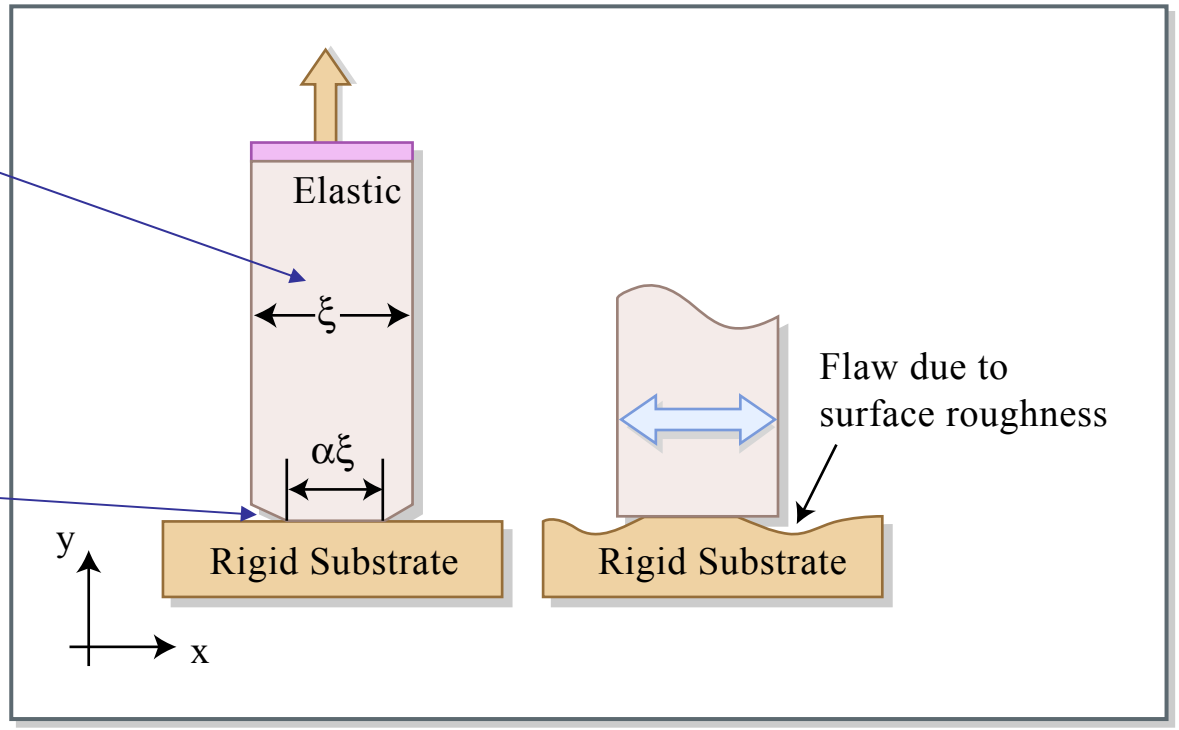

Figure by MIT OCW.

LJ: Autumn *et al*. have shown dispersive interactions govern adhesion of attachment in Gecko

Stress close to detachment as a function of adhesion punch size

Figure removed due to copyright restrictions.

$\sqrt{R_{cr} / R}$

Has major impact on adhesion strength:
At small scale no stress magnification

Smaller size leads to homogeneous stress distribution

Vary E and γ in scaling law

$$R_{cr} = \frac{8}{\pi} \frac{E^* \Delta\gamma}{\sigma_{th}^2}$$

The ratio

$$\sqrt{R_{cr} / R}$$

governs adhesion strength

Figure removed due to copyright restrictions.

- Results agree with predictions by scaling law
- Variations in Young's modulus or γ may also lead to optimal adhesion

Adhesion strength as a function of size

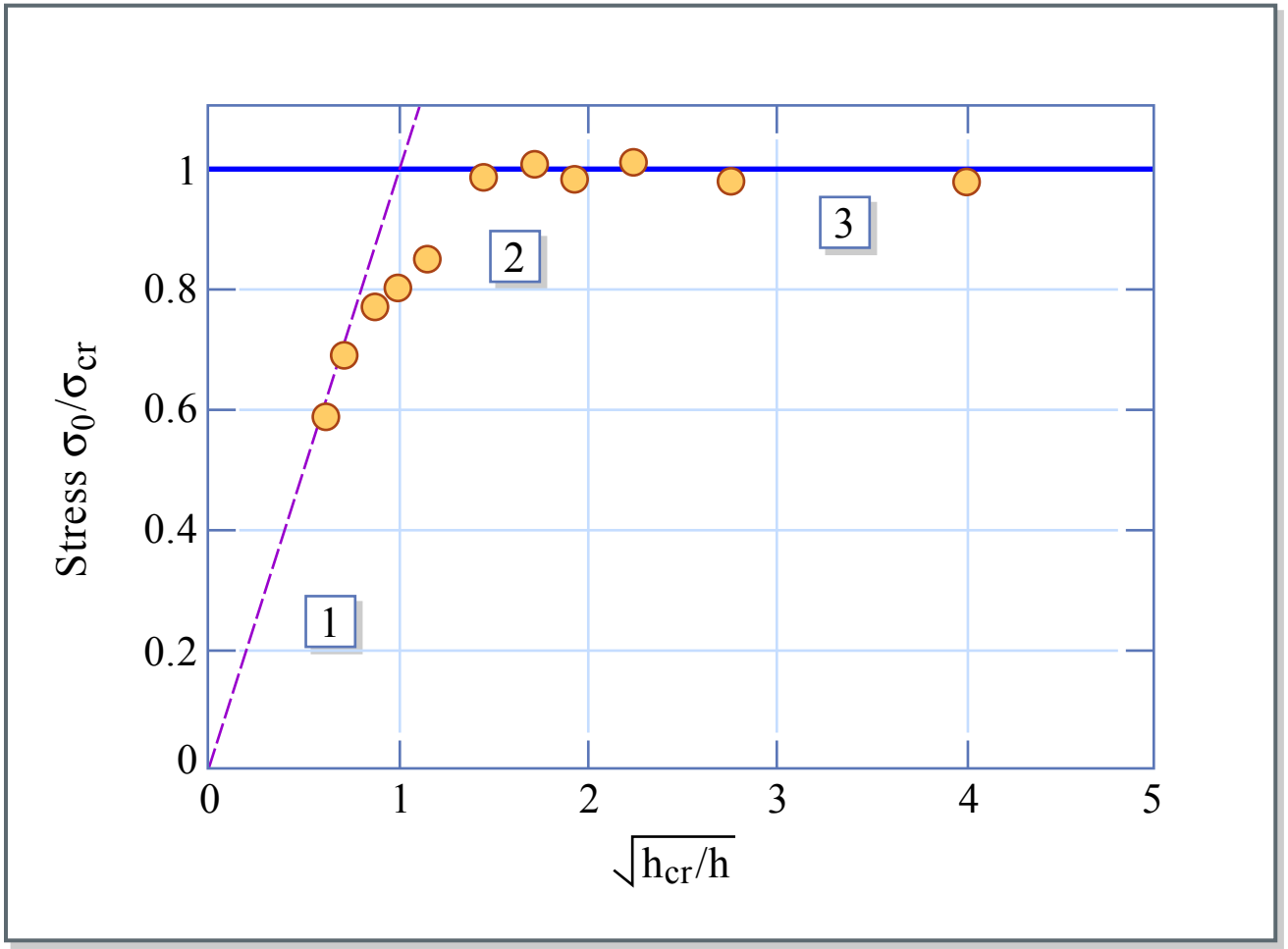

Figure by MIT OCW.

Optimal surface shape

Single punch

$$z = -\psi \frac{2\sigma_{th} R}{\pi E/(1-\nu^2)} \left[\ln\left(1-\bar{r}^2\right) + \bar{r} \ln\left(\frac{1+\bar{r}}{1-\bar{r}}\right) \right]$$

Concept:
Shape parameter ψ

Periodic array of punches

$$z = -\psi \frac{2\sigma_{th} R}{\pi E/(1-\nu^2)} \left\{ \left[\ln\left(1-\bar{r}^2\right) + \bar{r} \ln\left(\frac{1+\bar{r}}{1-\bar{r}}\right) \right] \right.$$

Images removed due to copyright restrictions.

$$- \sum_{n=1}^{\infty} \left[ln\left(\frac{(2n\lambda+\bar{r})^2 - 1}{(2n\lambda)^2 - 1}\right) + (2n\lambda+\bar{r}) ln\left(\frac{2n\lambda+\bar{r}+1}{2n\lambda+\bar{r}-1}\right) - 2n\lambda\, ln\left(\frac{2n\lambda+1}{2n\lambda-1}\right) \right]$$ PBCs

$$\left. - \sum_{n=1}^{\infty} \left[\ln\left(\frac{(2n\lambda-\bar{r})^2 - 1}{(2n\lambda)^2 - 1}\right) + (2n\lambda-\bar{r}) \ln\left(\frac{2n\lambda-\bar{r}+1}{2n\lambda-\bar{r}-1}\right) - 2n\lambda \ln\left(\frac{2n\lambda+1}{2n\lambda-1}\right) \right] \right\}$$

Derivation: Concept of superposition to negate the singular stress

Optimal shape predicted by continuum theory & shape parameter ψ

Figure removed due to copyright restrictions.

The shape function defining the surface shape change as a function of the shape parameter ψ. For $\psi=1$, the optimal shape is reached and stress concentrations are predicted to disappear.

Creating optimal surface shape in atomistic simulation

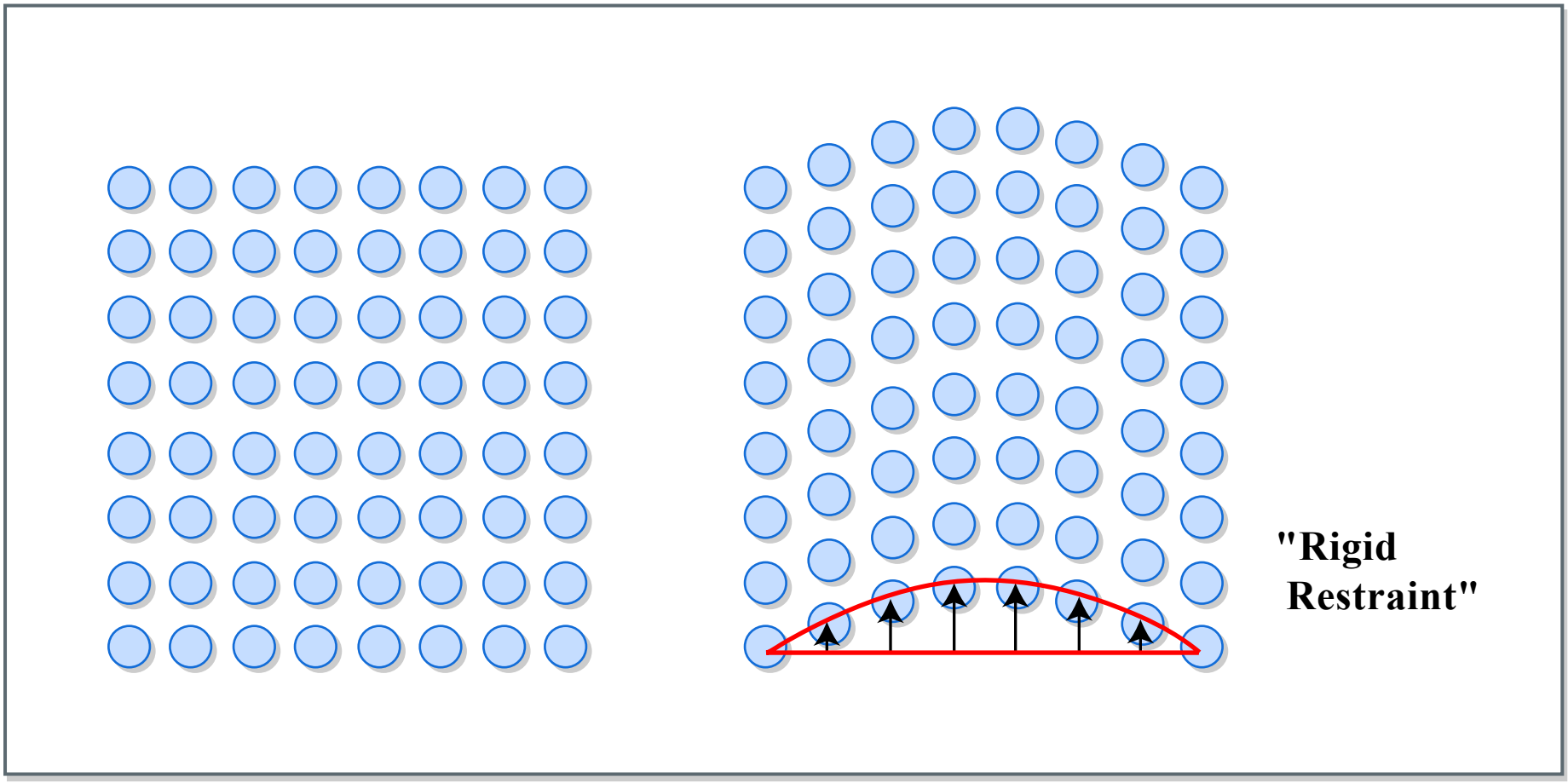

Figure by MIT OCW.

Strategy: Displace atoms held rigid to achieve smooth surface shape

Stress distribution at varying shape

Figure removed due to copyright restrictions.

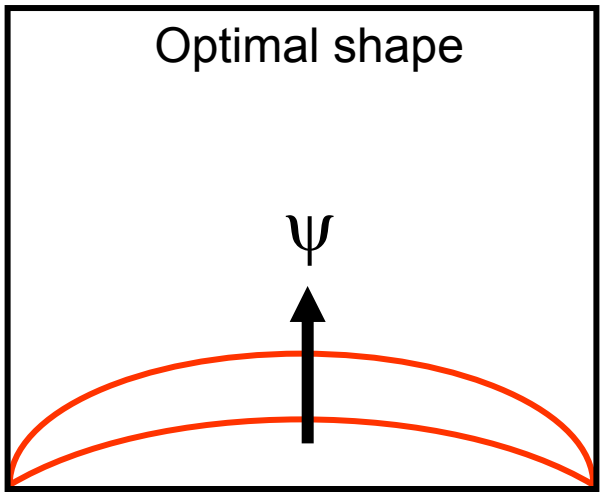

ψ=1: Optimal shape

Robustness of adhesion

Figure removed due to copyright restrictions.

- By finding an optimal surface shape, the singular stress field vanishes.
- However, we find that this strategy does not lead to robust adhesion systems.
- For robustness, shape reduction is a more optimal way since it leads to (i) vanishing stress concentrations, and (ii) tolerance with respect to surface shape changes.

Discussion and conclusion

- We used a systematic atomistic-continuum approach to investigate brittle fracture and adhesion at ultra small scales
- We find that Griffith's theory breaks down below a critical length scale
- Nanoscale dimensions allow developing extremely strong materials and strong attachment systems: **Nano is robust**

Small nano-substructures lead to robust, flaw-tolerant materials.
In some cases, Nature may use this principle to build strong structural materials.

- Unlike purely continuum mechanics methods, MD simulations can intrinsically handle stress concentrations (singularities) well and provide accurate descriptions of bond breaking
- Atomistic based modeling will play a significant role in the future in the area of modeling nano-mechanical phenomena and linking to continuum mechanical theories as exemplified here.

Chemical complexity: Modeling chemical reactions

Conventional molecular models

- **Empirical potentials**: Treatment of large molecular systems to capture inhomogeneities at nanoscale;
  >>10,000 atoms

  Dilemma: Many empirical potentials can not describe chemistry accurately (bond breaking, formation, …)

Images removed due to copyright restrictions.
Illustration of reaction: ethane to ethylene.

Nonreactive models: Require *a priori* knowledge of chemical state of atoms + connectivity: **Severely limits solution space**

Reactive force field: Concept

Nonreactive FF: $\phi = \frac{1}{2} k\left(r - r_0\right)^2$

"Harmonic spring"

r_0 EQ distance between atoms

k Spring constant

Constant valency (available bonds)

Images removed due to copyright restrictions.
Atomic bond model: bond analogous to a spring. Bonds between 2 sp3, sp2, and sp1 atoms.

Reactive FF: $\phi = \frac{1}{2} k(\mathrm{BO})\left(r - r_0(\mathrm{BO})\right)^2$

$$\mathrm{BO} = f(r)$$

Bond properties (bond stiffness k, EQ distance r_0) are made dependent on bond order (BO)

BO is function of bond distance (Pauling):
Theoretical link to quantum chemistry

Reactive versus non-reactive potential

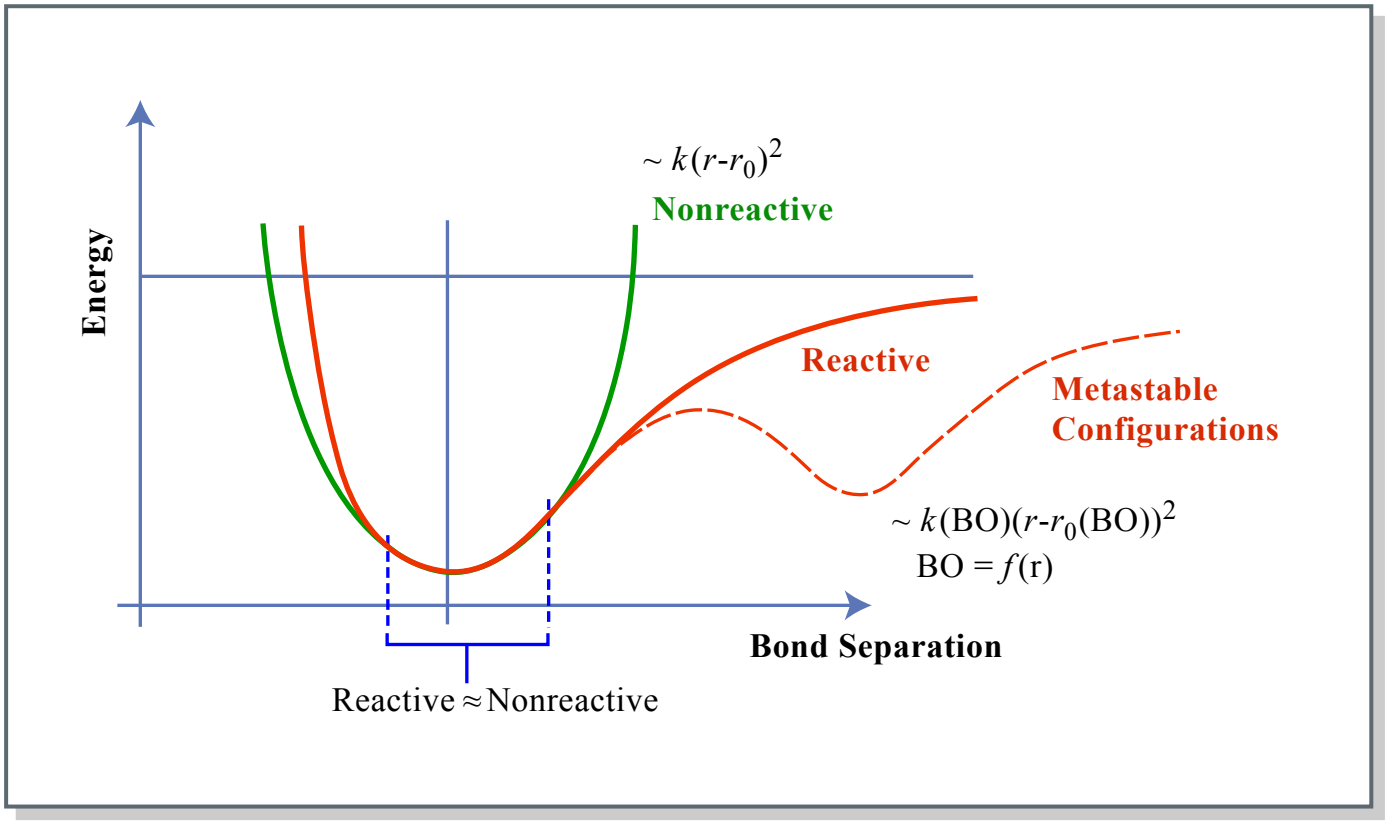

Figure by MIT OCW.

Difference between reactive and nonreactive model: Reactive model capable of describing energetics of small and large deviation from equilibrium (key during instabilities, chemical reactions..)

Figure by MIT OCW.

ReaxFF: Formulation

$$E_{system} = \underbrace{E_{bond} + E_{vdWaals} + E_{Coulomb}}_{\textit{2-body}} + E_{val,angle} + E_{tors}$$

3-body *4-body*

$$+ \underbrace{E_{over} + E_{under}}_{\textit{multi-body}}$$

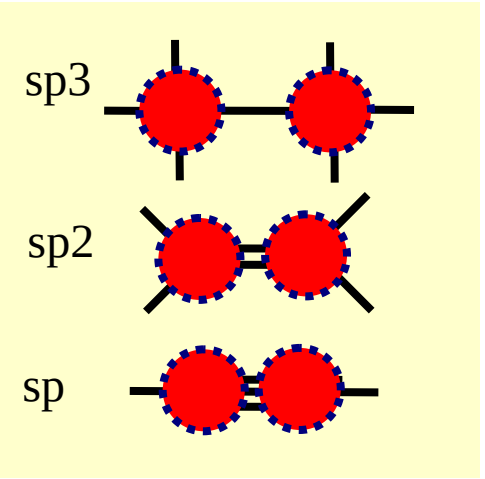

- A **bond length/bond order relationship** is used to obtain smooth transition (Pauling) from **non-bonded to single, double, and triple bonded systems**.
- All connectivity-dependent interactions (*i.e.* valence and torsion angles) are made **bond-order dependent**: Ensures that their energy contributions disappear upon bond dissociation
- Feature **non-bonded interactions** (van der Waals, Coulomb): **Shielded**
- ReaxFF uses a geometry-dependent **charge calculation scheme** (similar to QEq) that accounts for polarization effects
- Many parameters in the formulation have **physical meaning**

Charge equilibration

Images removed due to copyright restrictions.
Molecular models with each atom's charge labeled, comparing ReaxFF-calculated charges with actual.

Charges in ReaxFF are not fixed, but can flow, depending on local environment:

- Assign one electronegativity and hardness to each element; optimize these parameters against QM-charge distributions
- Use system geometry in solving electronegativity equilibration equations in every iteration

A. Duin *et al.*, 2001-2006

ReaxFF is highly transferable model

Image removed due to copyright restrictions.
Periodic table showing which elements can be described by ReaxFF; these elements are: H, He, Li, B, C, N, O, F, Ne, Na, Mg, Al, Si, P, S, Cl, Ar, K, Ca, Ti, V, Fe, Co, Ni, Cu, Zn, Se, Rb, Y, Zr, Mo, Ru, Te, Pt, an Bi.

Published ReaxFF force fields for:

- H/C (van Duin, Dasgupta, Lorant and Goddard, JPC-A 2001, **105**, 9396; van Duin and Sinninghe Damste, Org. Geochem.2003, **34**, 515; Chen, Lusk, van Duin and Goddard PR-B 2005, **72**, 085416, Han, Kang, Lee, van Duin and Goddard Appl. Phys. Lett. 2005, **86**, 203108)
- Si/SiO2/SiC (van Duin, Strachan, Stewman, Zhang, Xu and Goddard, JPC-A 2003, **107**, 3803; Chenoweth, Cheung, van Duin, Goddard and Kober, JACS 2005, **127**, 7192; Buehler, van Duin and Goddard, PRL 2006, **96**, 095505)
- Nitramines/RDX/TATP (Strachan, van Duin, Chakraborty, Dasupta and Goddard, PRL 2003,**91**,09301; Strachan, van Duin, Kober and Goddard, JCP 2005,**122**,054502; Han, Strachan, van Duin and Goddard, in preparation; van Duin, Dubnikova, Zeiri, Kosloff and Goddard, JACS 2005, **127**, 11053)
- Al/Al2O3 (Zhang, Cagin, van Duin, Goddard, Qi and Hector, PRB 2004,**69**,045423)
- Ni/Cu/Co/C (Nielson, van Duin, Oxgaard, Deng and Goddard, JPC-A 2005, **109**, 493)
- Pt/PtH (Ludwig, Vlachos, van Duin and Goddard, JPC-B 2006)
- Mg/MgH (Cheung, Deng, van Duin and Goddard, JPC-A 2005, **109**, 851)
- BN-nanotubes (Han, Kang, Lee, van Duin and Goddard, JCP 2005, **123**,114703; Han, Kang, Lee, van Duin and Goddard, JCP 2005, **123**,114704)
- Li/LiC (Han, van Duin and Goddard, JPC-A 2005, **109**, 4575)

A. Duin et al., 2001-2006

How is the ReaxFF model developed?

Image removed due to copyright restrictions.

Idea: Use concept of handshaking or overlap: Calculate set of properties with QM and ensure that ReaxFF reproduces these properties

Computational expense

Image removed due to copyright restrictions.
Graph showing that ReaxFF is 1,000,000 times faster than QM (DFT).

A. Duin et al., 2001-2006

Concurrent multi-scale simulations

Concurrent integration of various scales and paradigms

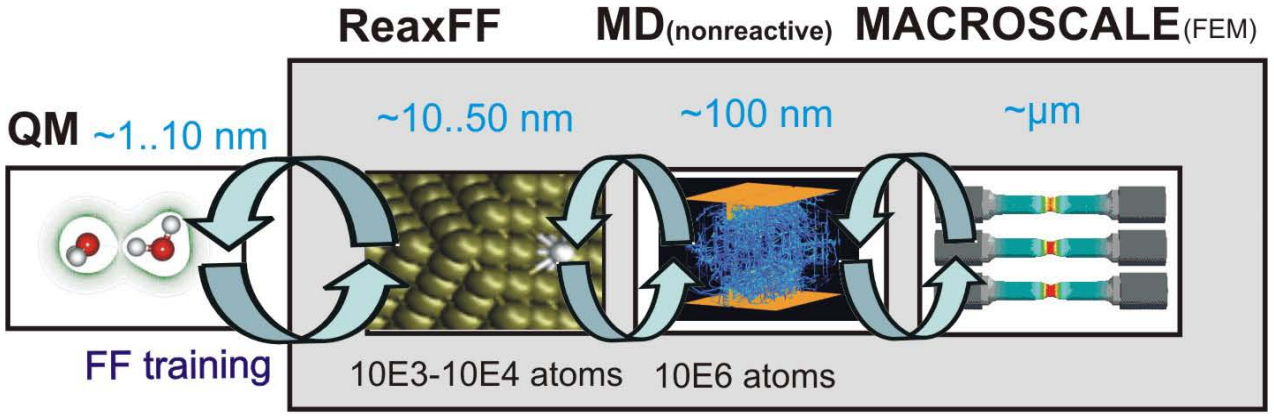

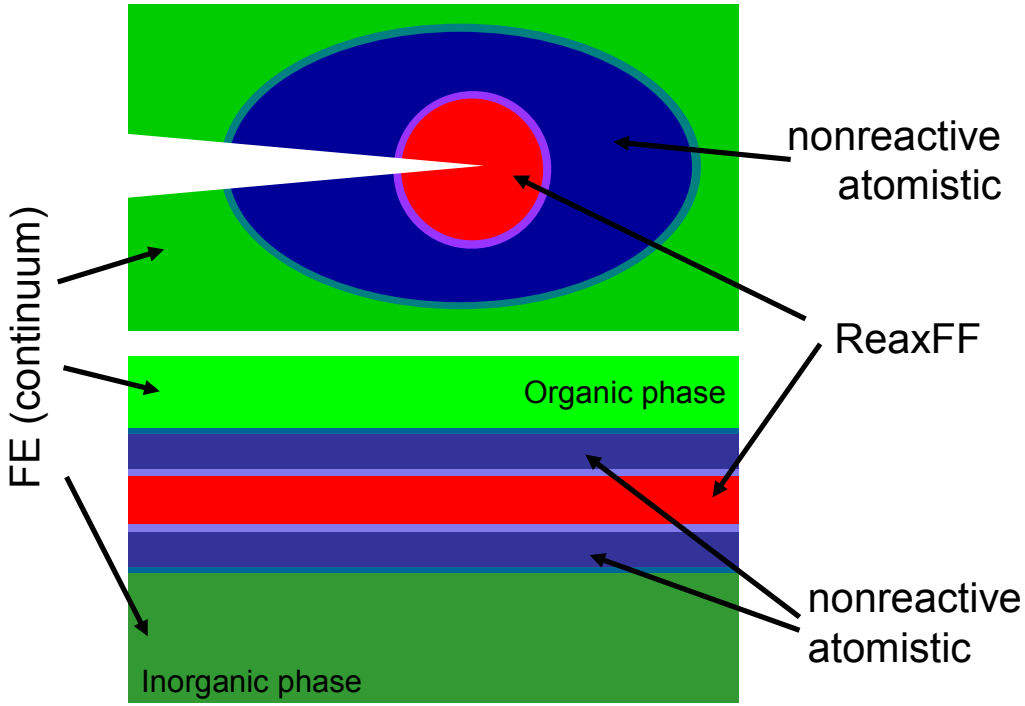

- Concurrent FE-atomistic-ReaxFF scheme in a crack problem (crack tip treated by ReaxFF) and an interface problem (interface treated by ReaxFF).
- Highlighted transition regions as handshake domains between different scale and methods.

M.J. Buehler, 2006, unpublished

Example for potential coupling: Concept of mixed Hamiltonian ("handshake")

- Developed scheme to couple different codes with each other based on weights describing the amount of force and energy contribution of different force engines: Works well for certain force fields

$$\sum_{i=0\ldots N} w_i = 1$$

$$\vec{F}_j = \sum_{i=0\ldots N} \vec{F}_{j,i} w_i$$

Images removed due to copyright restrictions.

See figs. 1, 2, 3, 4 and 5 in Buehler, Markus J., Adri C. T. van Druin, and William Goddard III. "Multiparadigm Modeling of Dynamical Crack Propagation in Silicon Using a Reactive Force Field." *Phys Rev Lett* 96 (2006): 095505-1 - 4.

Oxidation of a metal (Al) surface

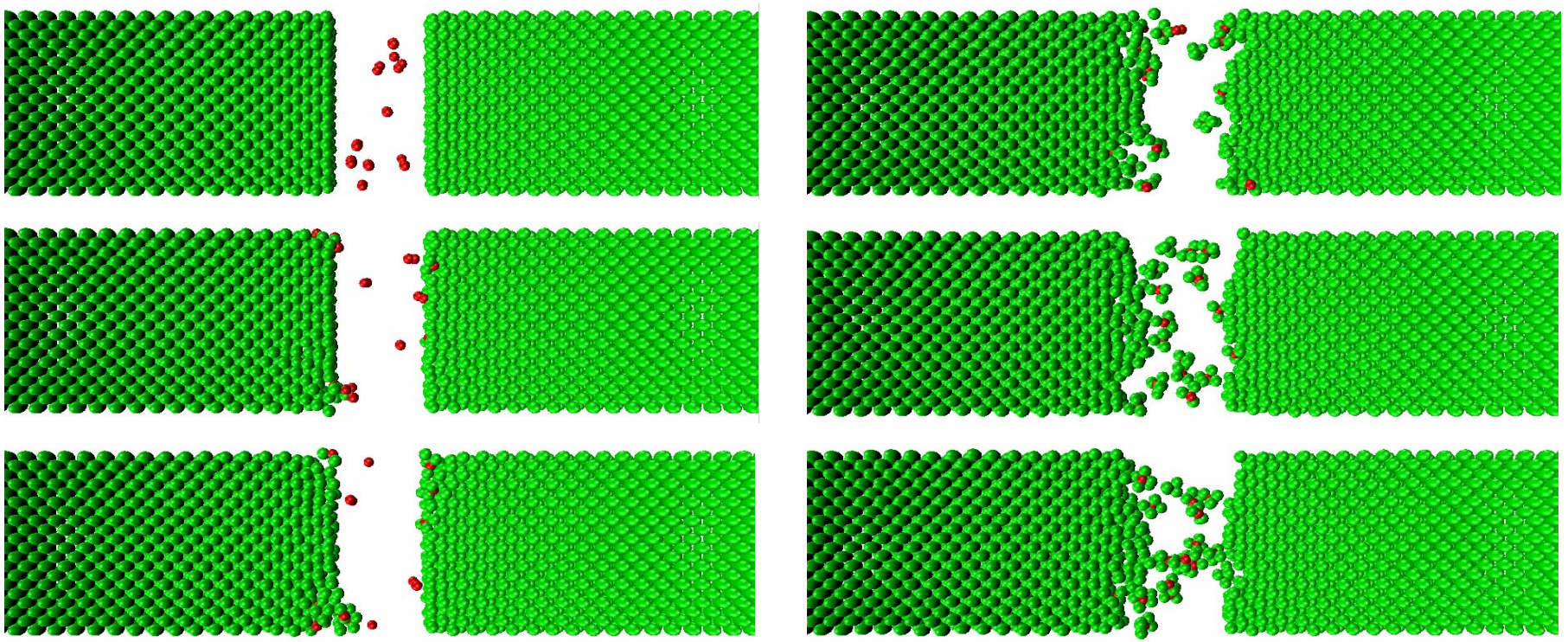

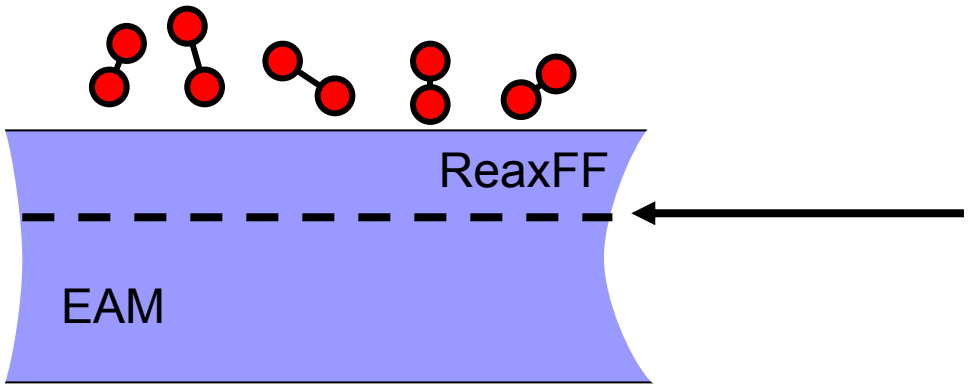

Reactive region expands during simulation
Based on determination of reaction front

M.J. Buehler, 2006, unpublished

Oxidation of a metal (Al) surface

- Examples demonstrates the concept of the moving boundary between different computational engines
- Boundary location determined by position of oxygen atoms: Automatic update

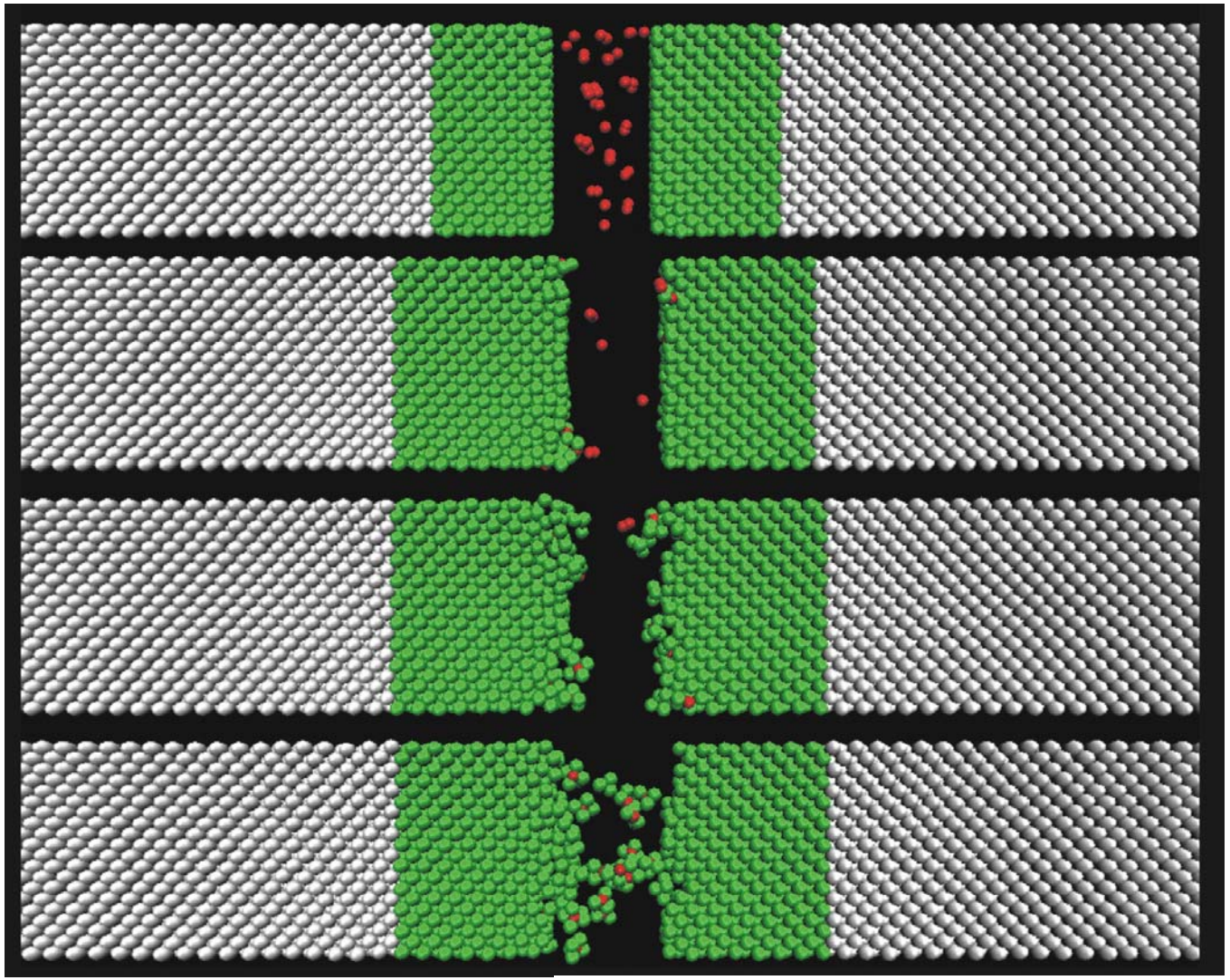

M.J. Buehler, 2006, unpublished

Metal/metal oxide systems

Al/Al-O system

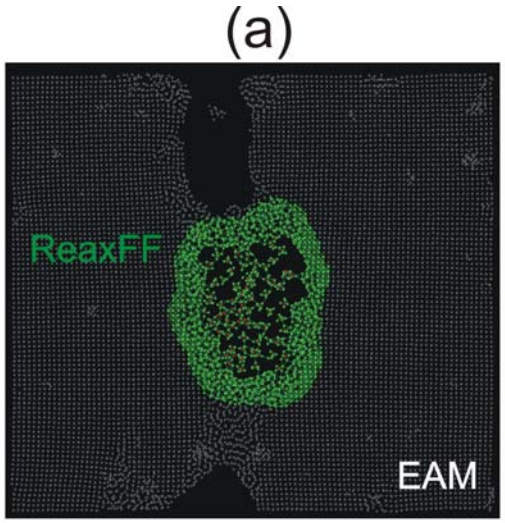

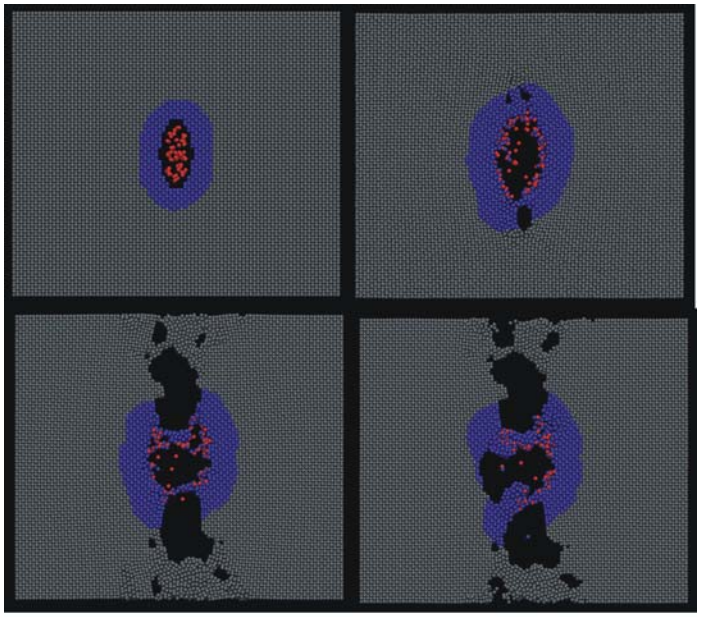

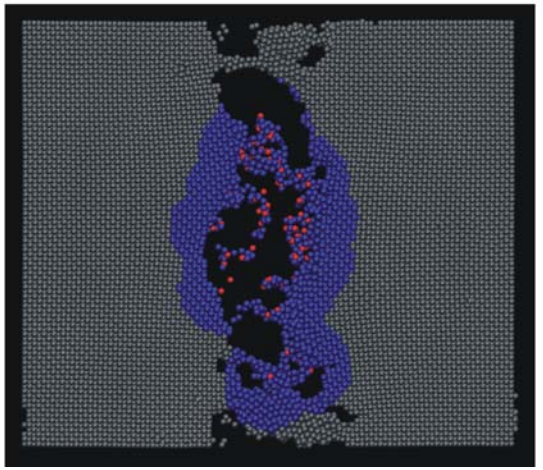

Ni/Ni-O system

M.J. Buehler, 2006, unpublished

Dynamic fracture of silicon:
Hybrid multi-paradigm modeling of crack initiation, propagation and fracture instabilities

Handshaking: Application to fracture

Images removed due to copyright restrictions.

See figs. 1, 2, 3, 4 and 5 in Buehler, Markus J., Adri C. T. van Druin, and William Goddard III. "Multiparadigm Modeling of Dynamical Crack Propagation in Silicon Using a Reactive Force Field." *Phys Rev Lett* 96 (2006): 095505-1 - 4.

- We consider a crack in a single silicon crystal under remote mode I loading.
- We use periodic boundary conditions in the *z* direction corresponding to a plane strain case.

- The smallest system contains 13,000 atoms and the largest system over 110,000 atoms.
- In the largest system, $L_x \approx 550$ Å and $L_y \approx 910$ Å.
- The number of reactive atoms varies between 500 and 3,000.
- Calculation of forces and energies in the reactive region is the most expensive part

Buehler *et al*., *Phys. Rev. Lett*., 2006

Reactive versus non-reactive potential

Images removed due to copyright restrictions.

See figs. 1, 2, 3, 4 and 5 in Buehler, Markus J., Adri C. T. van Druin, and William Goddard III. "Multiparadigm Modeling of Dynamical Crack Propagation in Silicon Using a Reactive Force Field." *Phys Rev Lett* 96 (2006): 095505 -1 - 4.

(110 crack surface)

.

• Crack propagation with a pure Tersoff potential (left) and the hybrid ReaxFF-Tersoff scheme (right) along the [110] direction (energy minimization scheme).
• The snapshots are both taken with the same loading applied and after the same number of minimization steps. The systems contain 28,000 atoms and $L_x \approx 270$ Å and $L_y \approx 460$ Å.

Shows importance of large-strain properties as suggested earlier (Buehler *et al*., Nature, 2003, Buehler and Gao, Nature, 2006)

Buehler *et al*., *Phys. Rev. Lett*., 2006

Cracking in Silicon: Model within CMDF

• To model cracking in Silicon more efficiently, we developed a multi-paradigm scheme that combines the Tersoff potential and ReaxFF

• The ReaxFF region is moving with the crack tip (region determined based on local atomic strain)

New hybrid scheme within CMDF

(110) crack surface, 10 % strain

Reactive region is moving with crack tip

Images removed due to copyright restrictions.

See figs. 1, 2, 3, 4 and 5 in Buehler, Markus J., Adri C. T. van Druin, and William Goddard III. "Multiparadigm Modeling of Dynamical Crack Propagation in Silicon Using a Reactive Force Field." *Phys Rev Lett* 96 (2006): 095505 -1 - 4.

ReaxFF
Tersoff

• CMDF reproduces experimental results (e.g. Cramer, Wanner, Gumbsch, 2000)

Buehler *et al*., *Phys. Rev. Lett*., 2006

Crack orientation dependence

Images removed due to copyright restrictions.

See figs. 1, 2, 3, 4 and 5 in Buehler, Markus J., Adri C. T. van Druin, and William Goddard III. "Multiparadigm Modeling of Dynamical Crack Propagation in Silicon Using a Reactive Force Field." *Phys Rev Lett* 96 (2006): 095505 -1 - 4.

Crack Speed as a function of Loading

Image removed due to copyright restrictions.
Graph illustrating jump in crack speed at critical strain.

Comparison: Experimental results

Image removed due to copyright restrictions.

See fig. 2 in Bernstein, N. and D. W. Hess.
"Lattice Trapping Barriers to Brittle Fracture."
Phys Rev Lett 91 (2003): 025501.

SW/EDIP can not reproduce this phenomenon

(Bernstein & Hess, *Phys. Rev. Lett.*, 2003)

Direct comparison with experiment

SW/EDIP can not reproduce this phenomenon, CMDF can!

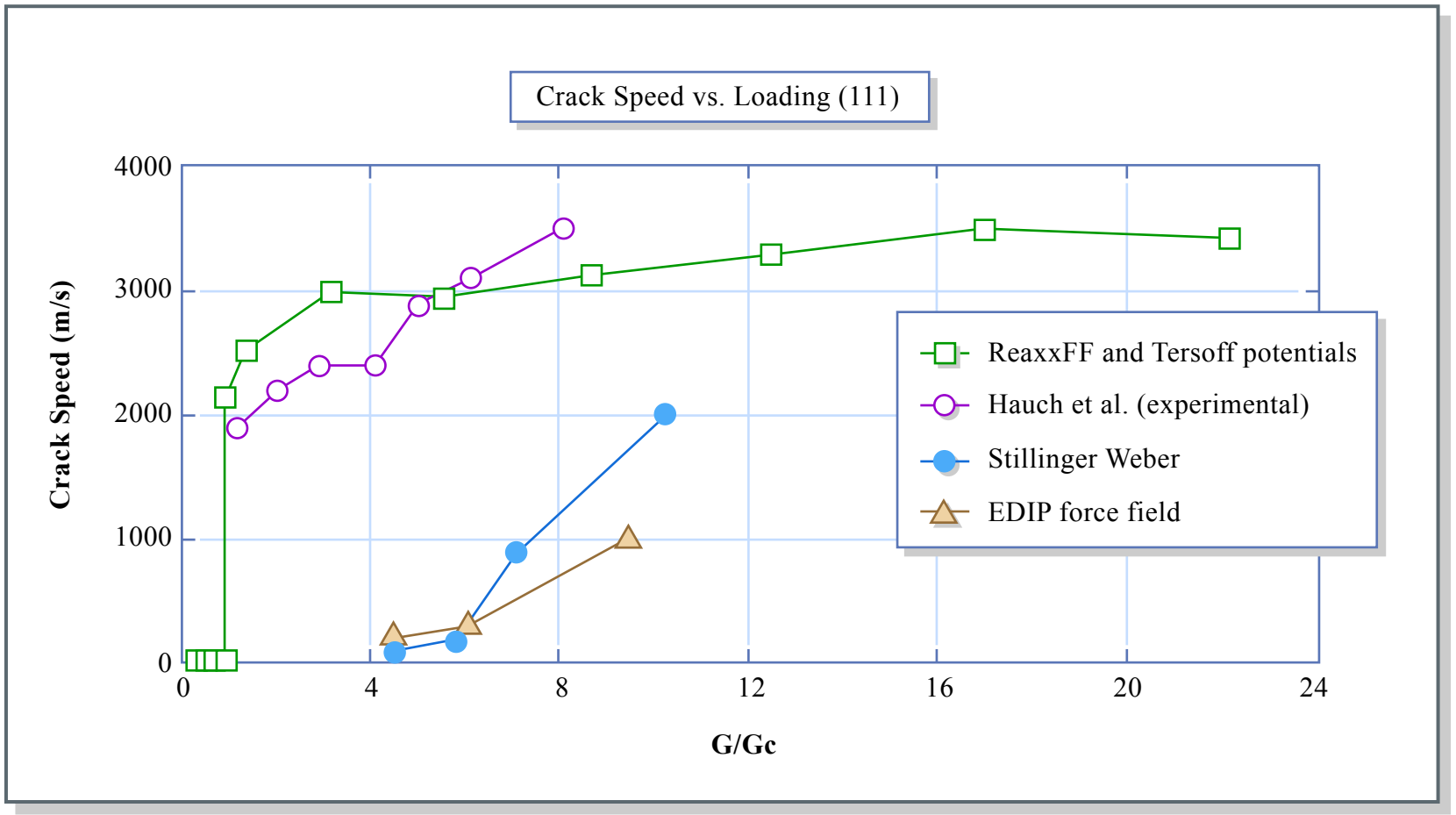

Figure by MIT OCW.

Tang, Buehler *et al.*, 2006

Atomistic mechanisms at onset of fracture

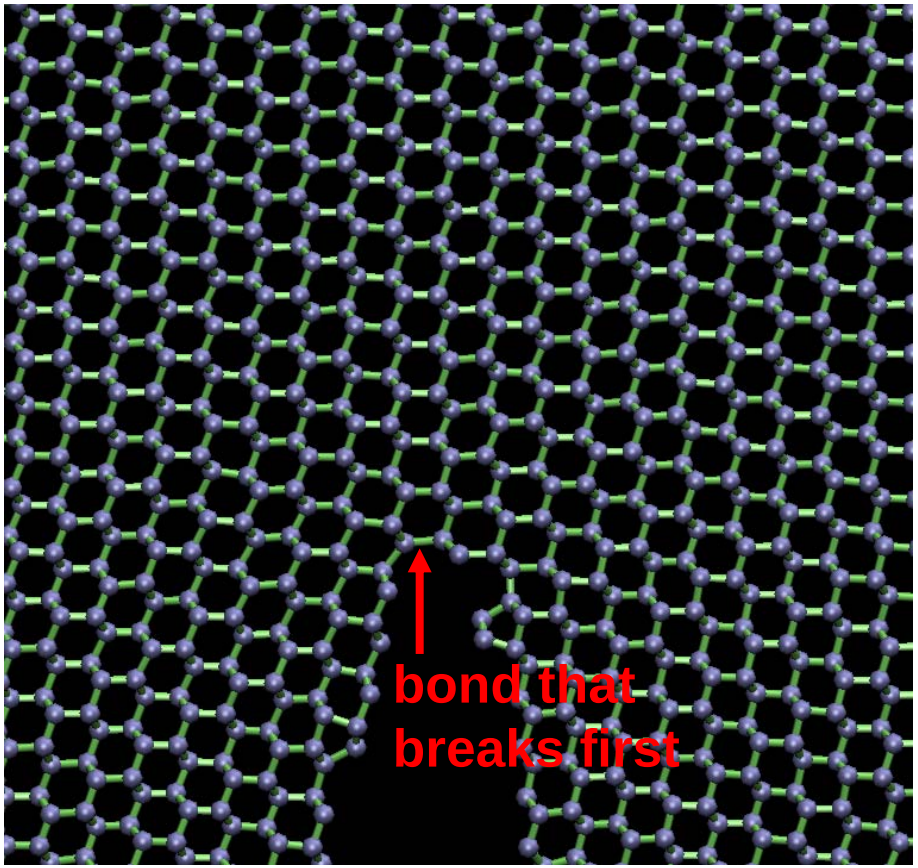

Initial crack structure

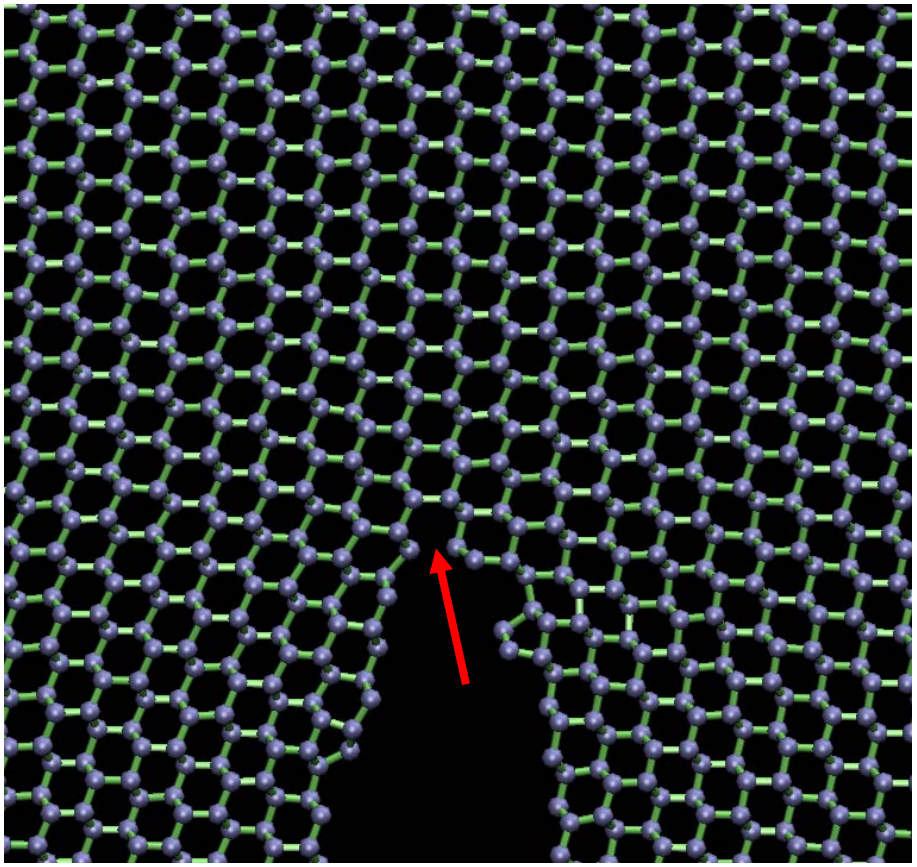

Breaking of first 6-membered ring

Atomistic mechanisms at onset of fracture: Formation of 5-7 rings

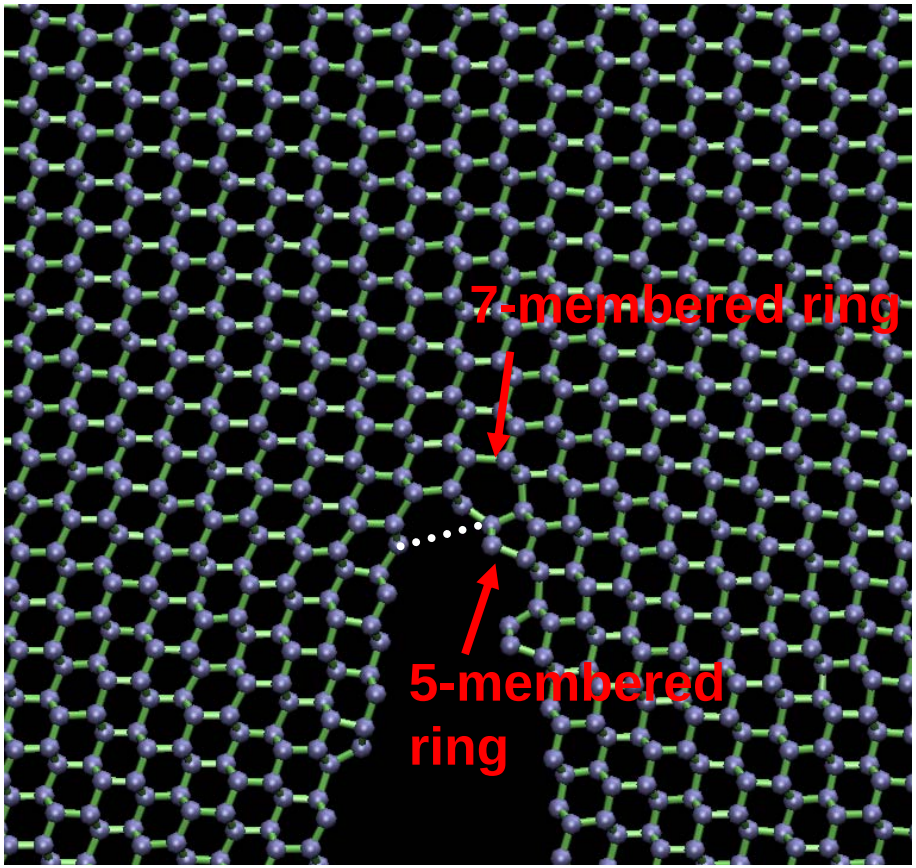

Formation of 7-5-ring combination

Also observed in TB calculations by Gabor Csanyi (Cambridge Univ.)

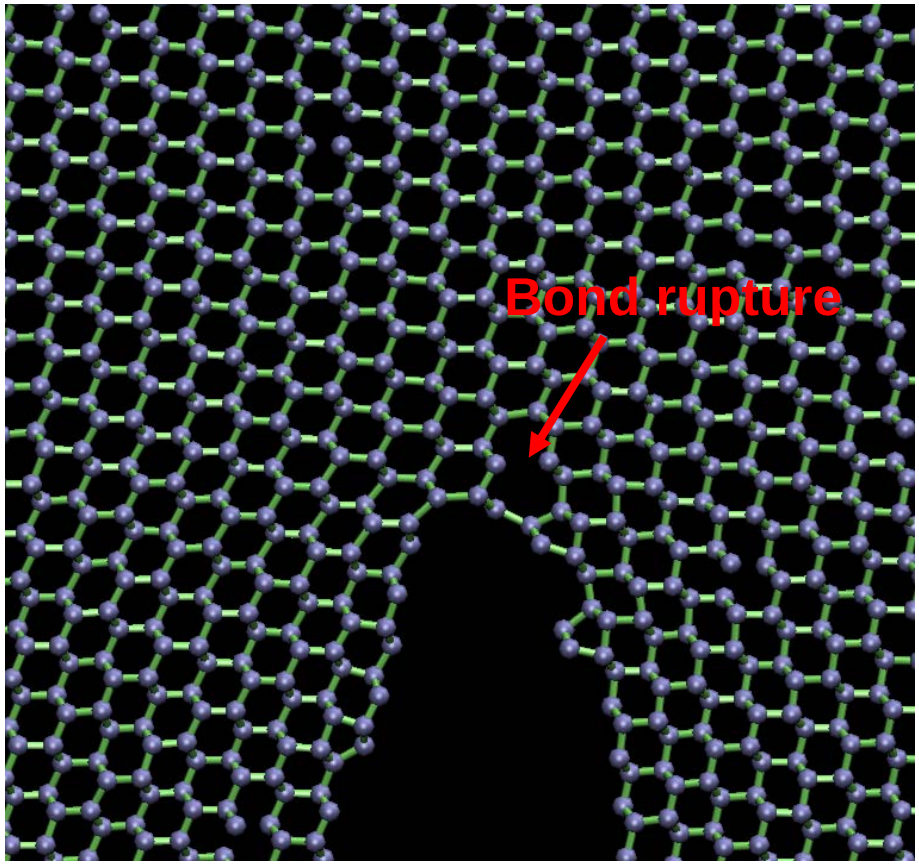

Rupture occurs ahead of 7-membered ring ("micro-crack")

Atomistic mechanisms at onset of fracture

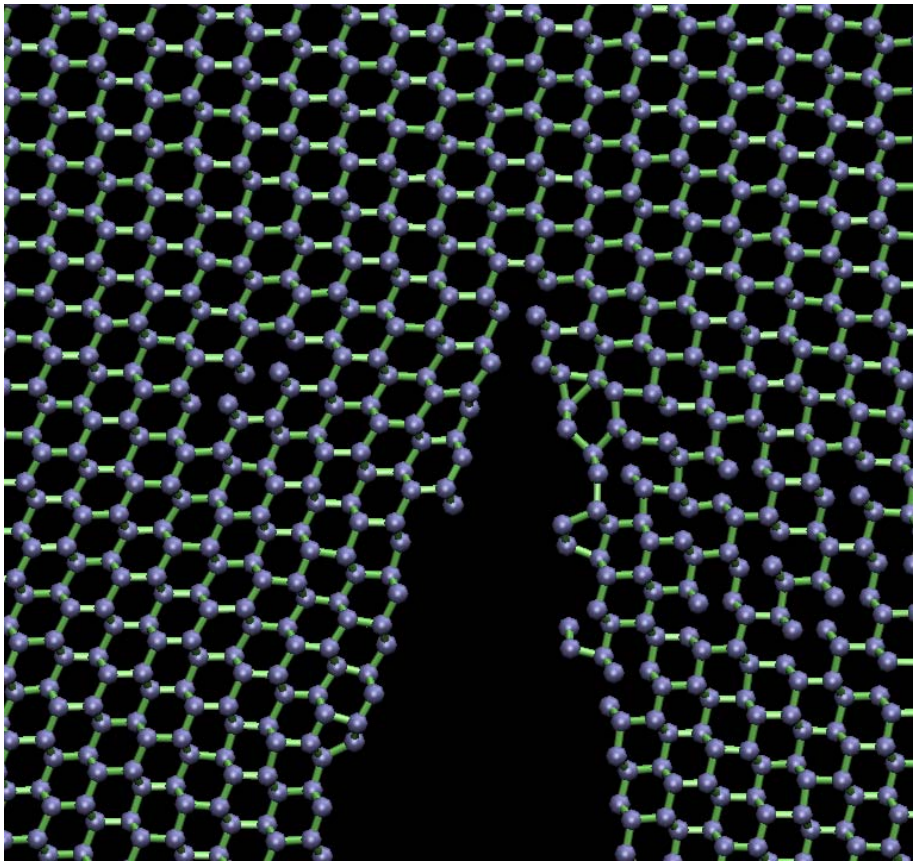

Crack propagation
(creates smooth surface)

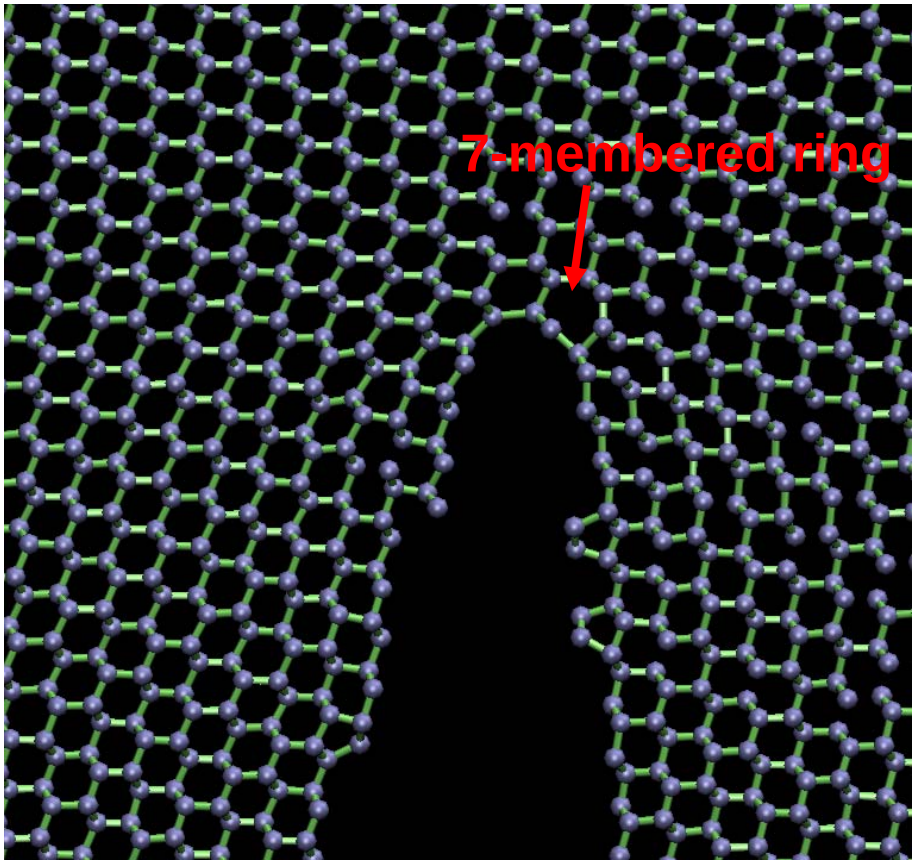

While crack propagates, formation of another 7-5 ring combination

Atomistic mechanisms at onset of fracture

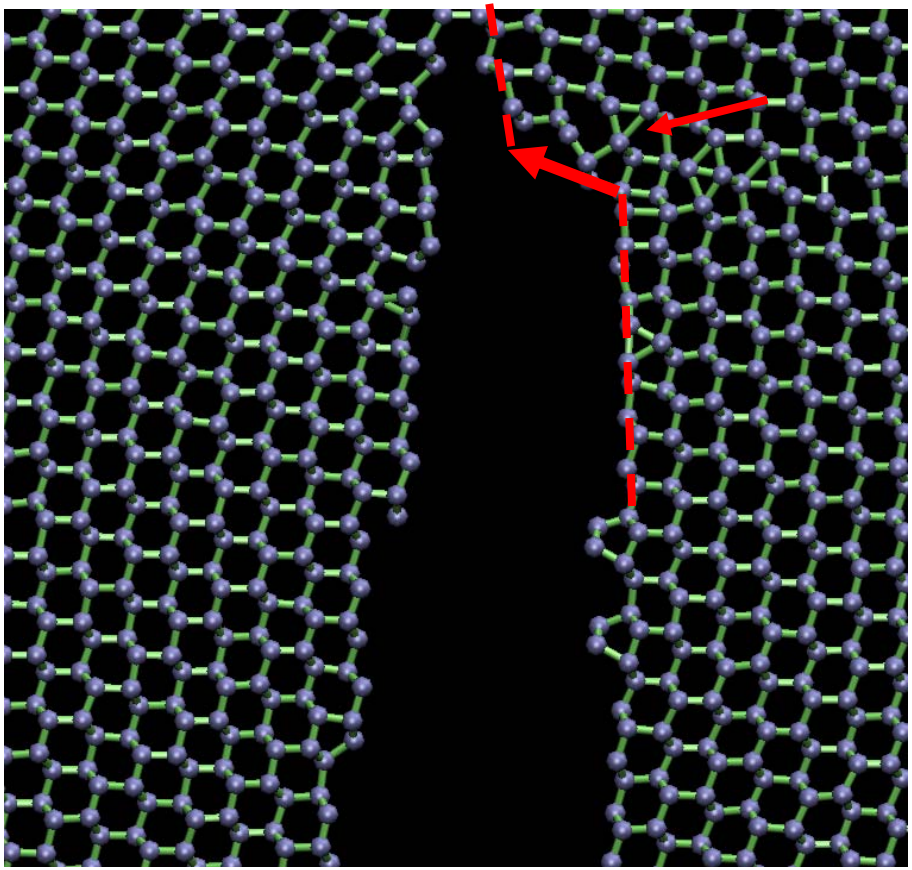

5-7 ring combination leads to change in crack direction, creating a slight surface step

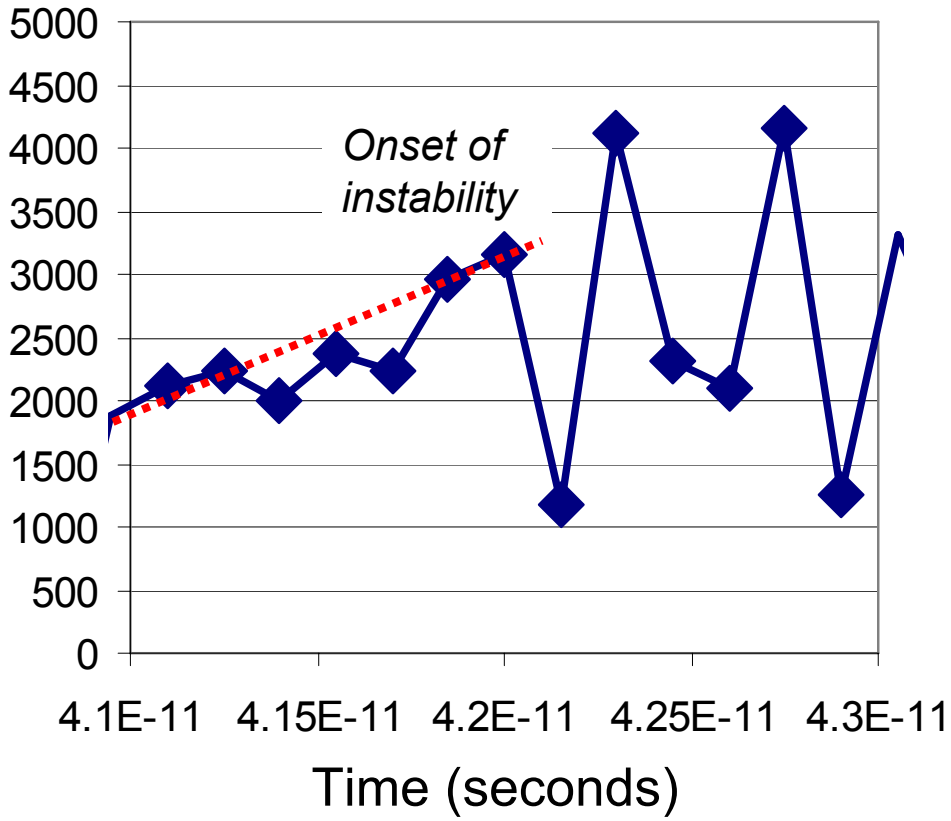

Instability sets in at ~66% of Rayleigh wave speed (assume c_R~4.5 km/sec)

Close to experimental observation

Atomistic mechanisms at onset of fracture

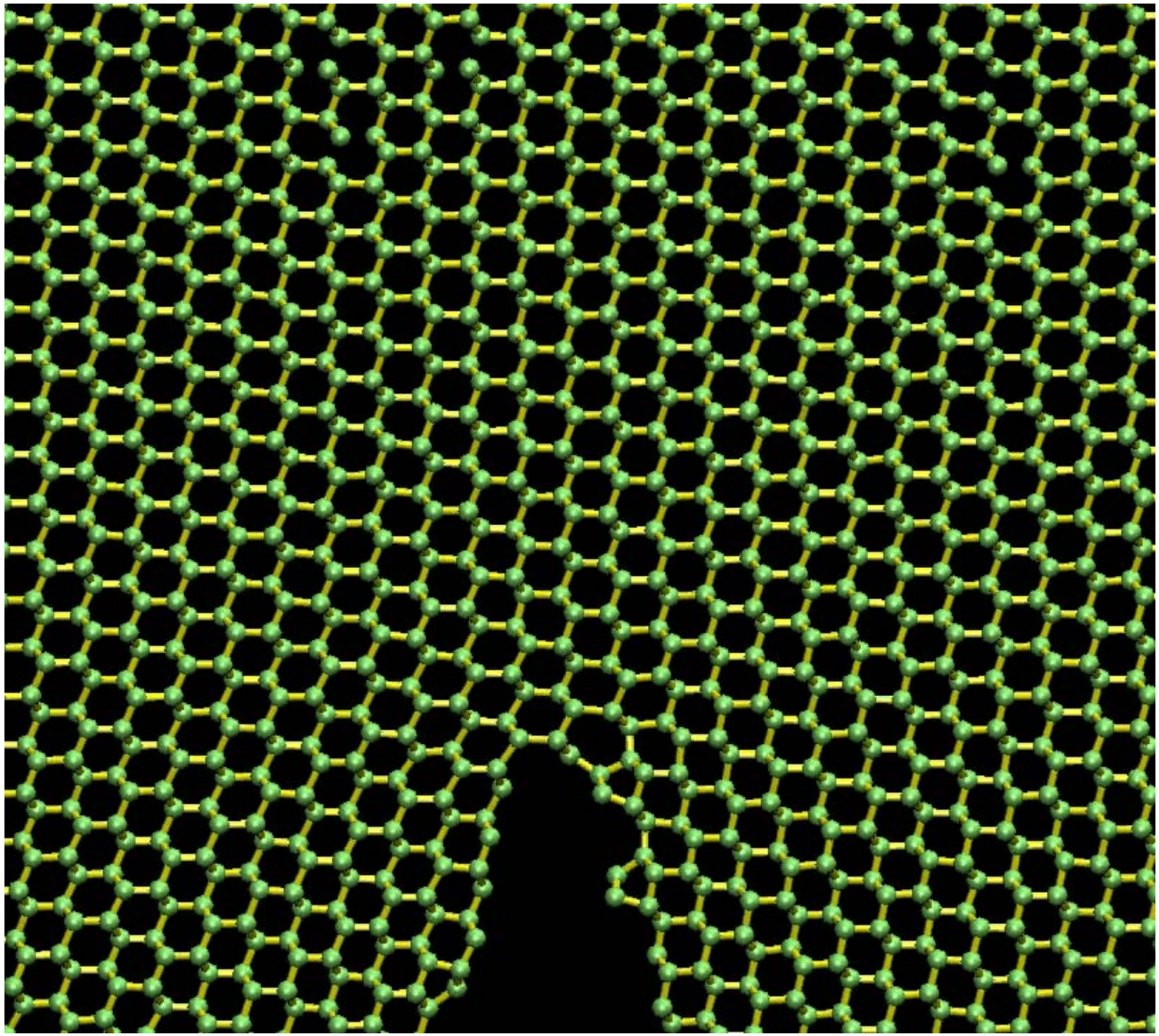

Oxidation versus brittle fracture

Images removed due to copyright restrictions.

See figs. 1, 2, 3, 4 and 5 in Buehler, Markus J., Adri C. T. van Druin, and William Goddard III. "*Multiparadigm Modeling of Dynamical Crack Propagation in Silicon Using a Reactive Force Field.*" Phys Rev Lett 96 (2006): 095505 -1 - 4.

- Crack dynamics in silicon without (subplots (a) and (c)) and with oxygen molecules present (subplots (b) and (d))
- Subplots (a) and (b) show the results for 5 percent applied strain, whereas subplots (c) and (d) show the results for 10 percent applied strain.
- The systems contain 13,000 atoms and $Lx \approx 160$ Å and $Ly \approx 310$ Å.

Buehler *et al*., *Phys. Rev. Lett*., 2006

Nanocrystalline materials

Fundamental length scales in nanocrystalline ductile materials

- Similar considerations as for brittle materials and adhesion systems apply also to ductile materials

- In particular, the deformation mechanics of nanocrystalline materials has received significant attention over the past decade

  • Strengthening at small grain size (Hall-Petch effect)

  • Weakening at even smaller grain sizes after a peak

http://me.jhu.edu/~dwarner/index_files/image003.jpg

Images removed due to copyright restrictions.

http://www.sc.doe.gov/bes/IWGN.Worldwide.Study/ch6.pdf

Hall-Petch Behavior

- It has been observed that the strength of polycrystalline materials increases if the grain size decreases

- The Hall-Petch model explains this by considering a dislocation locking mechanism:

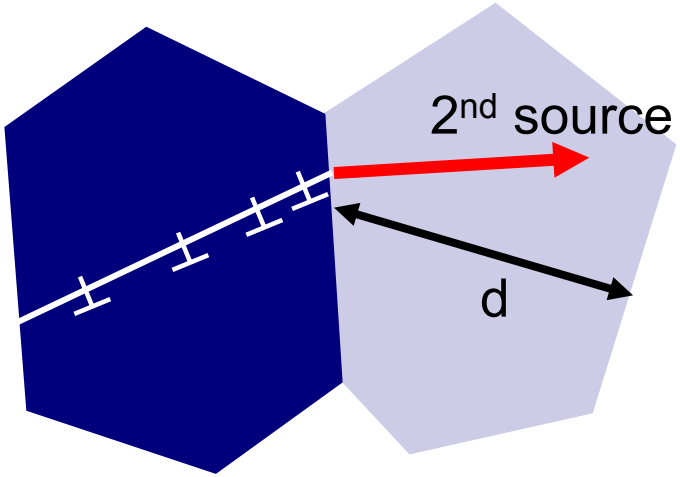

Nucleate second source in other grain (right)

Physical picture: Higher external stress necessary to lead to large dislocation density in pileup

$$\sigma_Y \sim \frac{1}{\sqrt{d}}$$

See, e.g. Courtney, Mechanical Behavior of Materials

The strongest size: *Nano is strong!*

Different mechanisms have been proposed at nanoscale, including

- GB diffusion (even at low temperatures) – Wolf *et al*.
- GB sliding – Schiotz *et al*.
- GBs as sources for dislocations – van Swygenhoven, stable SF energy / unstable SF energy (shielding)

Figure removed due to copyright restrictions.
See p. 15 of http://www.imprs-am.mpg.de/summerschool2003/wolf.pdf

Yamakov *et al*., 2003, Schiotz et al., 2003

Deformation in nanocrystalline materials

- **Review articles:**

  Yamakov V, **Wolf D**, Phillpot SR, et al.
  Deformation-mechanism map for **nanocrystalline** metals by molecular-dynamics simulation
  NATURE MATERIALS 3 (1): 43-47 JAN 2004

  Van Swygenhoven H, Derlet PM, Froseth AG
  Stacking fault energies and slip in **nanocrystalline** metals
  NATURE MATERIALS 3 (6): 399-403 JUN 2004

- **Controversial debate about the mechanisms at ultra small scales**
  - Wolf *et al.*: Coble creep as deformation mechanism
  - Van Swygenhoven and Schiotz suggest dislocation mechanisms to be active even to small grain sizes (even full dislocations) and grain boundary sliding or short range atomic rearrangements in the grain boundary